

DEPARTMENT OF MINES AND ENERGY
SOUTH AUSTRALIA

REPT.BK.NO. 87/92
BROAD VIEW 1 DDH WELL-
COMPLETION REPORT

GEOLOGICAL SURVEY

by

L.R. RANKIN

and

R.B. FLINT
REGIONAL GEOLOGY

JULY, 1987

DME.151/87

<u>CONTENTS</u>	<u>PAGE</u>
ABSTRACT	1
INTRODUCTION	1
PREVIOUS INVESTIGATIONS	3
WELL HISTORY	3
General	3
Drilling Data	
GEOLOGY	5
Drillhole Orientation	5
Drilling Results	6
Summary of Petrography	6
a) Mt. Shannan Iron Formation	6
b) Bosanquet Formation	10
Structure	13
GEOCHEMISTRY	14
Igneous Geochemistry	14
Economic Potential	15
GEOPHYSICS	16
Neutron, Gamma and Bulk Density Logs	16
Resistivity	17
Magnetic Susceptibility	18
SUMMARY AND STRATIGRAPHIC IMPLICATIONS	18
Summary	18
Stratigraphic Implications	19
APPENDIX I - THIN SECTION DESCRIPTIONS	
APPENDIX II - PLATES	
APPENDIX III - GEOCHEMICAL DATA	

LIST OF FIGURES

	<u>Plan No.</u>
1. Location of Broad View 1 DDH.	S19321
2. Outcrop geology of Broad View 1 DDH area.	S19322
3. Plot of deviation with depth for Broad View 1 DDH.	S19323
4. Summary geological log of Broad View 1 DDH.	87-540
5. a) Zr/Ti vs Nb/Y and b) SiO ₂ vs Zr/Ti diagrams for deformed volcanics of the Bosanquet Formation, Myola Volcanics, Tidnamurkana Volcanics and McGregor Volcanics. The igneous discrimination fields are adapted from Floyd and Winchester (1978).	S19325

6. Zr vs Sr vs Rb triangular diagram for deformed volcanics of the Bosanquet Formation, Myola Volcanics and Tidnamurkana Volcanics. S19326
7. a) AFM and b) Al_2O_3 vs Fe_2O_3 vs MgO triangular diagrams for deformed volcanics of the Bosanquet Formation, Myola Volcanics, Tidnamurkana Volcanics and McGregor Volcanics. S19327
8. a) SiO_2 vs TiO_2 and b) Rb vs Sr vs Ba diagrams for deformed volcanics of the Bosanquet Formation, Myola Volcanics, Tidnamurkana Volcanics and McGregor Volcanics. S19328
9. Chondrite-normalised diagram for deformed volcanics of the Bosanquet Formation, Myola Volcanics, Tidnamurkana Volcanics and McGregor Volcanics. Each trend is an average of all available samples for each formation. S19329
10. Histogram plots of base metal concentrations within the Bosanquet Formation and Mount Shannan Iron Formation. S19331
11. Natural gamma, neutron, bulk density, magnetic susceptibility and geological logs for Broad View 1 DDH. 87-464
12. Resistivity logs for Broad View 1 DDH. 87-465

DEPARTMENT OF MINES AND ENERGY
SOUTH AUSTRALIA

RPT. BOOK NO. 87/92
DME.NO. 151/87
DISK NO. 91

BROAD VIEW 1 DDH WELL COMPLETION REPORT

ABSTRACT

SADME Broad View 1 DDH intersected 381.6 m of deformed and recrystallised porphyritic rhyolite-rhyodacite with minor interlayered calcsilicate gneiss, and 170.8 m of Bosanquet Formation (new name) metasedimentary calcsilicate gneisses and schists, and magnetite+grunerite-rich horizons (Mount Shannan Iron Formation member of the Hutchison Group). This sequence of deformed volcanics plus minor calcsilicates has not been previously recognised in the Early Proterozoic stratigraphy of the Gawler Craton. Detailed petrographic and microstructural analysis, as well as geochemical comparisons to other Early Proterozoic acid volcanics have not allowed unambiguous determination of the stratigraphic position of this unit.

Although base-metal values for both the Mount Shannan Iron Formation and the Bosanquet Formation within the drillcore are low, the presence of acid volcanics associated with carbonate-rich metasediments, with minor occurrences of sulphides, is an encouraging target for base-metal exploration.

INTRODUCTION

Mapping of the Archaean-Early Proterozoic rocks of the Gawler Craton on the KIMBA 1:250 000 sheet (Flint and Rankin, in prep.) located a sequence of poorly-outcropping calcsilicates approximately 5 km E of Carappee Hill. The calcsilicates vary from coarse-grained, diopside-rich and containing abundant clasts of dolomite, rhyolite, granite and quartzite to fine-grained varieties with no clasts. They occur on both the western and eastern sides of a ridge containing float of magnetite quartzite (assumed Upper Middleback Jaspilite), however no contact relationships are exposed. The calcsilicates trend approximately 175° and dip 85°E.

The units lie in a region of very-poor outcrop, with subcropping Mangalo Schist and Lincoln Complex gneisses to the east, and in the west Tertiary laterite which suggests the presence of either the Upper or Lower Middleback Jaspilites of the Hutchison Group.

Broad View 1 (Bore General File unit no. 6131002SW00124) was proposed by the Regional Geology Branch in June 1986 and subsequently spudded on 2nd August 1986. The aims of the drilling project were:

1. To drill a stratigraphic section from the calcsilicate gneisses and suspected acid volcanics into the nearby suspected iron formation. This would aid recognition of the stratigraphic position of the calcsilicates, which were thought to be either Hutchison Group metasediments or metasediments and volcanoclastics associated with the younger Myola or McGregor Volcanics. It was important to clarify this stratigraphy, as no acid volcanics or volcanoclastics have previously been recognised within the Hutchison Group.
2. To test the economic potential of this unit for base metal mineralisation. Pb/Zn mineralisation associated with calcsilicates and massive carbonates (of the Hutchison Group) has been discovered at Menninie Dam by Billiton Aust. (Higgins and Hellsten, 1986). The possible presence of acid volcanics in the sequence was encouraging as an indication of a potential exhalative source of base metal sulphides.

To address both these aims, Broad View 1 was spudded near the centre of the calcsilicate+(?)volcanic unit and drilled towards 257° at an initial depression angle of 60° in an attempt to provide a section across the western half of the calcsilicate unit.

PREVIOUS INVESTIGATIONS

Very little work has been conducted in the immediate area of the calcsilicate gneisses. Kerr McGee drilled 12 RAB holes in the area, ranging from 20 to 63 deep. The exploration target was uranium mineralisation in the Quaternary/Tertiary sediments, with no success. Bottom-hole lithologies were described as schist, quartzite and granite gneiss.

Billiton Aust., in joint venture with CRA undertook intensive exploration to the south of the calcsilicates, in the area of the Campoona Syncline. The exploration target was stratiform Pb/Zn mineralisation within the Hutchison Group metasediments. Minor mineralisation was found within schists and calcsilicate gneisses. The outcropping calcsilicates to the north (in the vicinity of Broad View DDH 1) were largely ignored in these exploration programs (Weeden, 1982).

WELL HISTORY

General

Well Name

South Australian Department of Mines and Energy Broad View 1

Location

Latitude 33° 25'

Longitude 136° 19'

5 km east of Carapsee Hill, Eyre Peninsula.

Map References

1:250 000 KIMBA SH 53-7

1:100 000 Kimba 6131

S.A. Department of Mines and Energy Unit Number

6131002SW00124

Elevation

Ground Level : 200 m

Total Depth

578.6 m

Drilling

Commenced 31/7/86

Completed 23/10/86

Drilling Number

S.A. Department Mines and Energy
 Drilling and Engineering Services
 Dalgleish St
 Thebarton

Driller

F. Costello

Drilling Rig

Mindrill 10L DD No. 6

Construction Details

Hole collared at surface with plunge 60° towards 257°

Om to 2.20 m -	215.90 mm roller bit and set 203.2 mm PVC to 2.20 m
2.20 m TO 2.90 m -	HQ, no core
2.90 m to 12.00 m -	197 mm Hawthorne blades and set 152 mm PVC to 12.00 m
12.00 m to 26.00 m -	140 mm roller bit and set 101.6 mm steel pipe to 26.00 m.
26.00 m to 139.20 m -	HQ coring 113.20 m core recovered 113.20m. Cased with HQ rods to 139.20 m.
139.20 m to 316.5 m -	NQ coring 177.3 m, core recovered 177.3m. Cased with NQ rods to 316.5 m.
316.5 m to 578.66 m -	BQ coring 262.16 m, cored recovered 262.16 m.

All rods used as casing removed, with 20m of 101.6 mm pipe unable to be removed.

Tropari Survey

On completion of the hole, five readings of plunge and azimuth were taken by tropari. Results are:

Depth	Plunge	Azimuth
100m	54°	270°
200m	40°	268°
300m	33°	264°
366m	21°	268°
528m	18°	319°

Comments

Thirty two core bits were used for 553.36m of core, averaging 17.29m/bit. Numerous mechanical delays were encountered during drilling, including replacement of the main gear box three times, failure of the input shaft and drive bearings in the auxillary gear box, and overhaul of the fuel injectors on site.

GEOLOGY

Drillhole Orientation

Exposed calcsilicates, near the drillhole, strike 167° and dip 70° to the East. To maximise the stratigraphic thickness, the drillhole should ideally have been drilled perpendicular to the layering within the calcsilicates, i.e. 20° towards 257°. However the shallowest depression angle permissible for the rig is 60°, so the hole was collared with an orientation of 60° plunge towards 257°.

Orientation of the drillhole varied considerably during drilling (Fig. 3). The trend remained relatively constant, varying a little more to the west (270°). Plunge of the drillhole systematically decreased from 60° to 20°, finishing almost perpendicular to the layering within the calcsilicates. The change in drillhole orientation was beneficial; a cored stratigraphic interval of 440 m was obtained rather than an estimated 300 m (assuming a constant depression angle of 60°).

Drilling Results

Broad View 1 was drilled to a total depth of 578.6 m intersecting 26 m of Cainozoic fluviatile sediments and 552 metres of Early Proterozoic metasediments and metavolcanics (Fig. 4). The Early Proterozoic sequence has been divided into two units; a calcsilicate and iron-formation metasedimentary sequence correlated with the Mount Shannan Iron Formation of the Hutchison Group (Duncan, 1976; Parker and Lemon, 1982), and a predominantly metavolcanic sequence with minor metasediments. This latter sequence has not been previously recognised within the Early Proterozoic stratigraphy of the Gawler Craton, and has been named the Bosanquet Formation (Rankin and Flint, in prep.). The following descriptions of the two formations are based on detailed logging of the drillcore and petrographic descriptions of 70 thin sections.

The deformational nomenclature $D_{1,2}$ etc. used in this report corresponds to that used by Parker and Lemon (1982) for the Kimban Orogeny.

Summary of Petrography

a) Mount Shannan Iron Formation

The drillhole intersected 170.8 m of poorly- to well-banded calcsilicate and magnetite-rich schists and gneisses (from 578.6 m to 407.8 m). Five principal lithologies were recognised in drillcore:

- 1) streaky-foliated calcsilicate schist/gneiss.
- 2) poorly-banded calcsilicate gneiss.
- 3) quartz+feldspar+biotite schist/gneiss.
- 4) well-banded calcsilicate.
- 5) magnetite-rich iron formation.

The contacts between these units are typically gradational and subjective, with complex interlayering of the units on various scales from 1 cm to several metres.

1) Streaky-foliated calcsilicate.

This unit consists of interlayered fine- to medium-grained schists and gneisses with a variable-intensity streaky foliation/schistosity in hand specimen. The mineralogy of the calcsilicate varies considerably between layers on both a micro- and mesoscopic scale. Dominant mineral assemblages include:

calcite+biotite+hornblende.

calcite+hornblende+diopside.

calcite+magnetite+grunerite+diopside (+quartz).

biotite+hornblende+magnetite+spinel.

biotite+actinolite/hornblende+grunerite+magnetite.

Layers of biotite+calcite schist (Plate 1) up to 2 m thick are common within the streaky calcsilicate unit, with an intense schistosity defined by the preferred-dimensional orientation of biotite. The schistosity is intersected at a moderate angle (40°) by a weak fabric defined by a second-generation growth of medium-grained biotite. The streaky appearance of the foliation is produced by a strong anastomosing of the biotite layering around attenuated, medium-grained aggregates of calcite. Bent deformation twins are rare in the calcite. Medium-grained poikiloblastic hornblende grains are common, with partial replacement by biotite. Minor subhedral epidote is a rare accessory. Within the calcite+amphibole-rich layers, the amphibole varies from blue-green actinolitic hornblende (Plate 2) to colourless to pale-brown grunerite. Grunerite is typically associated with fine-grained magnetite+medium-grained quartz. The amphiboles have typically replaced diopside, which occurs as anhedral relic grains within decussate clusters of prismatic amphibole grains.

2) Poorly-banded calcsilicate gneiss.

This unit consists of massive to poorly-banded, fine- to coarse-grained marbles and calcsilicate gneisses (Plates 3, 4) with minor thin (<5 cm) bands of biotite-rich schist. The weak compositional banding is typically contorted and occasionally

disrupted. A weak to moderate foliation in thin section is defined by the preferred-dimensional orientation of medium-grained biotite, which is partially replaced by chlorite. Mineral assemblages include:

calcite+biotite/chlorite (+magnetite + grunerite).
 calcite+biotite/chlorite+quartz+diopside+actinolite.
 calcite+actinolite+chlorite.

Tight folds occur within calcite+biotite marble layers, with a weak axial-planar foliation defined by fine-grained magnetite+grunerite+biotite. Diopside typically occurs as coarse-grained poikiloblasts within quartz-rich layers adjacent to calcite layers. Actinolite has partially replaced diopside, forming decussate clusters of acicular to prismatic grains.

3) Quartz+feldspar+biotite schist/gneiss.

This unit consists of fine-grained, granoblastic-elongate gneiss and schist, with minor medium-grained microcline megacrysts within a matrix of fine-grained quartz+microcline+biotite+minor plagioclase. The megacrysts are lenticular and elongate parallel to an intense, layer-parallel foliation. Some megacrysts have fine-grained coronas of microcline and minor inclusion-rich plagioclase, possibly due to metasomatic recrystallisation. Fine-grained biotite-rich schist layers contain abundant fine-grained acicular sillimanite and fine- to medium-grained anhedral pyrite. Within the biotite-rich layers, a weak second foliation oblique to the principal foliation is defined by a second generation of fine-grained biotite. Fine-grained muscovite partially overprints both generations of biotite. Accessory phases within this unit include calcite, diopside and sphene.

This unit is a fine-grained metasediment, the original lithology most likely being a lithic arkose.

4) Banded calcsilicate schist/gneiss.

This unit exhibits the greatest variation in mineralogy on both a microscopic and mesoscopic scale of layering, and is distinctive in core with well-developed compositional banding between pale-grey calcite-rich and dark green-grey amphibole-rich layers. Mineral assemblages within different layers include:

calcite+biotite+quartz+garnet+magnetite.
 quartz+actinolite/hornblende+calcite+biotite (\pm garnet).
 actinolite/hornblende+magnetite+grunerite+quartz+pyrite.
 quartz+biotite+hornblende+calcite.
 grunerite+garnet+biotite+magnetite+quartz
 biotite+quartz+calcite.
 calcite+actinolite/hornblende+diopside+magnetite
 quartz+magnetite+grunerite.

A moderate to strong foliation, parallel to the compositional layering, is defined by the preferred-dimensional orientation of biotite, elongate magnetite and occasionally actinolite/hornblende and grunerite.

The calcite-rich layers include impure marbles and calcite+biotite schist. Calcite typically exhibits deformation twinning and weakly serrate grain boundaries. The amphibole-rich layers have varied mineralogy and textures. The amphiboles grade from fine- to medium-grained actinolite and actinolitic hornblende to grunerite. Actinolite/hornblende is most commonly associated with calcite+biotite+diopside, while grunerite is most commonly associated with quartz+magnetite and biotite+garnet (Plate 5). The two amphiboles coexist in some specimens (Plates 6, 7), where calcsilicate layers contact fine-grained, granoblastic-elongate quartz+magnetite layers. Within these samples, the actinolite/hornblende tends to be weakly aligned to the foliation, or randomly orientated, while the grunerite occurs as a medium-grained band along the calcsilicate/quartzite contact, with the prismatic grains perpendicular to the contact (Plate 8). This suggests possible metasomatic growth of grunerite.

Medium- to coarse-grained diopside has been partially replaced by actinolite/hornblende, while poikiloblastic, medium- to coarse-grained iron-rich garnets have been partially replaced by grunerite. One specimen contains a layer of coarse-grained, boudinaged helicitic subhedral garnets, which have overgrown early generation folds. The folds are seen as trails of fine-grained opaques within the garnets, with an axial-planar fabric parallel to the layer-parallel foliation outside of the garnets (Plate 9). This suggests that the predominant garnet growth occurred after the D_1 foliation-forming deformation and possibly pre- D_2 deformation which was responsible for the macroscopic folding of the dominant foliation.

5) Iron Formation.

The distinction between the banded calcsilicates and this unit is gradational and subjective, depending on the abundance of magnetite. Two principal lithologies are incorporated into the iron formation unit; a magnetite quartzite (Plate 10) and a hornblende/grunerite+biotite+garnet+magnetite schist (Plate 11).

The magnetite quartzite consists of fine- to medium-grained granoblastic quartz with abundant fine-grained anhedral magnetite. Minor fine-grained grunerite occurs as acicular needles in "hourglass" aggregates roughly parallel to the foliation (Plate 12).

The amphibole schists contain abundant fine-grained magnetite associated with actinolitic hornblende (Plate 13), grunerite and garnet. Both lithologies are typically folded by tight to isoclinal folds on both a mesoscopic and microscopic scale.

b) Bosanquet Formation (new name)

The nature of the boundary at 407.8 m between metasediments of the Mt. Shannan Iron Formation and the Bosanquet Formation is not clear. Drillcore near this depth is very broken and corresponds to a zone of significant water loss during drilling. A discordancy of 8° in the orientations of the foliations also occurs near this depth. The boundary is apparently sharp, with abrupt termination of the iron-rich and calcium-rich lithologies of the Mount Shannan Iron Formation to

acid volcanics of the Bosanquet Formation. Stratigraphic facing of the units is not known, but the Bosanquet Formation is assumed to be either synchronous or younger than the Mount Shannan Iron Formation.

The Bosanquet Formation (407.8 m to 26.2 m) consists predominantly of metamorphosed and recrystallised rhyodacite, with minor interlayered calcsilicate and arkosic gneisses. The rhyodacite is divided into two main units: a megacrystic rhyodacite and a foliated rhyodacite.

1) Megacrystic rhyodacite.

This unit is found near the 'base' of the Bosanquet Formation, (from 400.33 m to 315.4m), and consists of coarse-grained (<2 cm), subhedral tabular microcline phenocrysts (Plate 14) and medium-grained, rounded, subequant quartz phenocrysts within a fine-grained matrix of quartz+feldspar+biotite (\pm zircon). The matrix is recrystallised, with a granoblastic-elongate to weakly anastomosing gneissic foliation. The microcline phenocrysts contain abundant inclusions and have suffered intense fracturing and boudinaging during the foliation-forming deformation. Subgrain and new-grain recrystallisation is common within the slightly attenuated megacrysts, and development of medium-grained quartz 'tails' within the megacryst strain shadows.

Quartz phenocrysts are typically medium-grained, sub - round to round, with weak to intense deformation-band and subgrain development (Plate 15). Many phenocrysts exhibit rims of polygonal subgrains and recrystallised new grains. Several quartz phenocrysts exhibit relic embayments (Plate 16), infilled with fine-grained recrystallised quartz+feldspar+biotite. The matrix most likely recrystallised from a microcrystalline or glassy volcanic groundmass. The evidence of dynamic recrystallisation seen within both the matrix and phenocrysts suggests that the foliation, developed during recrystallisation, is mylonitic in character.

2) Foliated rhyodacite

This is the dominant unit intersected in Broad View 1, and consists of a grey, well-foliated recrystallised rhyodacite with abundant quartz and minor microcline megacrysts. The unit differs from the megacrystic unit in both megacryst composition and size, content and intensity of tectonic fabric development. Quartz megacrysts range from subequant to lenticular with increasing foliation intensity (Plate 17), and exhibit intense deformation-band, subgrain and new-grain development. Microcline megacrysts are typically attenuated parallel to the foliation, fractured and partially recrystallised (Plate 18).

The matrix consists of fine-grained quartz+feldspar+biotite (\pm muscovite) (Plate 19), with quartz exhibiting minor sub-grain and deformation-band development and weakly lobate grain boundaries. These features suggest dynamic recrystallisation of the matrix during deformation. The microfabric of specimens with an intense foliation and a variable-intensity elongation lineation is protomylonitic to mylonitic in character, with abundant dynamic recrystallisation of both matrix and megacrysts. With increasing recrystallisation the foliation becomes anastomosing. The intensity and mylonitic character of the foliation becomes greater towards the top of the drillhole, suggesting the presence of a minor shear zone within the Bosanquet Formation immediately east of the drillhole.

3) Metasediments

Well-banded, grey to green calcsilicate gneisses occur as layers (0.2m-20m) within the metavolcanics. The calcsilicates are medium- to coarse-grained, granoblastic to granoblastic-elongate quartz+microcline+plagioclase+hornblende+biotite+calcite gneisses with a weak to intense foliation parallel to a well-developed compositional banding (Plate 20). The compositional banding is typically defined by alternating layers of biotite+quartz+ plagioclase and hornblende+calcite+quartz+ microcline. Diopside occasionally occurs as coarse-grained porphyroblasts partially replaced by actinolitic hornblende. Quartz and feldspar typically exhibit curved to lobate grain boundaries and weak internal deformation features. Coarse-grained, partially recrystallised microcline and quartz megacrysts are rare.

The unit is an interlayered sequence of calcareous and arkosic metasediments, deposited during quiescent periods within a cycle of acid volcanism. The presence of microcline and quartz megacrysts are likely to represent volcanoclastic input during sedimentation.

Structure

Two major foliation-forming events (D_1 and D_2) have been recognised within the drillcore, producing S_1 and S_2 respectively. D_1 and D_2 are interpreted as being the D_1 and D_2 regional events of the Early Proterozoic Kimban Orogeny of Parker and Lemon (1982).

The Mount Shannan Iron Formation metasediments have a weak to intense foliation (S_1) parallel to an original sedimentary layering (S_0). S_1 has been preserved within helicitic garnets, which have overgrown intrafolial F_1 microfolds with an axial-planar fabric (S_1) parallel to the S_{0-1} foliation surrounding the garnets. S_1 developed during upper amphibolite-facies metamorphism. The combined S_{0-1} foliation has been folded by tight to isoclinal, mesoscopic folds. Within the hinges of these folds, a weak- to moderate-intensity axial-planar foliation is defined by the preferred-dimensional orientation of biotite, quartz and/or magnetite (Plates 21, 22), plus minor muscovite. Within specimens without mesoscopic folds, S_2 varies from parallel to oblique to S_{0-1} . This suggests that the sequence is near the hinge/limb contact zone of a macroscopic, tight F_2 fold. This fold is most likely a synform, closing to the east of the drillhole. The development of S_2 occurred during slight metamorphic retrogression, with replacement of garnet and diopside by magnetite, biotite, grunerite and actinolitic hornblende.

The Bosanquet Formation rhyodacites have been recrystallised under amphibolite-facies metamorphism, with development of a weak- to moderate-intensity mylonitic foliation axial-planar to minor tight to isoclinal folds. The foliation in the rhyodacites is concordant to subcordant to the S_{1-2} foliation within the Mount Shannan Iron Formation, with a maximum angular discordancy near the contact of approximately 8° . This foliation is interpreted as S_2 . A weak muscovite foliation oblique to the

principal foliation within some specimens of the Bosanquet Formation may be either a late S_2 overprint associated with folding, or a weak S_3 foliation. The variable mylonitic character of the fabric within the deformed volcanics, as evidenced from dynamic recrystallisation microstructures, is probably due to heterogeneous localisation of shear strain during D_2 ductile deformation.

GEOCHEMISTRY

Sixty one samples of both the Bosanquet Formation and the Mount Shannan Iron Formation were submitted to AMDEL for selected trace-element analysis, and a further six samples of the Bosanquet Formation deformed volcanics were submitted for whole-rock silicate analysis. The geochemical data are tabulated in Appendix III.

Igneous Geochemistry

Known Early Proterozoic acid volcanics from the eastern Gawler Craton are the Myola Volcanics (and the equivalent Tidnamurkuna Volcanics in the Peake and Dension Inlier) and McGregor Volcanics. The Bosanquet Formation volcanics were compared to the Myola Volcanics, Tidnamurkuna Volcanics and McGregor Volcanics, using both mobile and immobile trace elements. (Nb/Y) vs (Zr/Ti) and SiO_2 vs (Zr/Ti) immobile element discrimination diagrams, developed by Floyd and Winchester (1978) for discrimination of altered and metamorphosed volcanics show that each volcanic suite occupies a separate field (Fig. 5). The Bosanquet Formation plots within the rhyodacite-dacite field on the (Nb/Y) vs (Zr/Ti) diagram, although an enrichment of Zr with respect to the Myola and Tidnamurkuna suites shifts the Bosanquet Formation into the trachyte and the comendite/pantellerite fields. This relative enrichment in Zr can also be seen in a plot of Zr vs Sr vs Rb. (Fig. 6). This enrichment of Zr within the Bosanquet Formation may be due to contamination of the parent magma with Zr-rich crustal sediments.

An AFM diagram and an Al_2O_3 vs Fe_2O_3 vs MgO diagram of the four suites (Fig. 7) indicate a slight enrichment in MgO with respect to the Myola and Tidnamurkuna suites, and a slight enrichment of alkalis with respect to the McGregor Volcanics.

The slightly higher MgO values for the Bosanquet Formation may be due to contamination from the contemporaneous, carbonate-rich metasediments.

Although some of the geochemical trends of the Bosanquet Formation are very similar to the Myola, Tidnamurkana and McGregor suites, (e.g. SiO_2 vs TiO_2 and Rb vs Sr vs Ba; Figs 8 a,b), the majority of discrimination diagrams suggest that the Bosanquet Formation is not directly comparable to the Myola, Tidnamurkana or McGregor Volcanics. This is supported by a chondrite normalised plot of trace elements (Fig. 9). The Myola, Tidnamurkana and McGregor suites plot relatively close to each other, while the Bosanquet Formation shows some differences, particularly with a depletion in La.

The geochemical data suggest that the Bosanquet Formation may not be related to the syn-Kimban volcanic events represented by the Myola Volcanics (dated at $1791 \pm 4\text{Ma}$), Tidnamurkana Volcanics ($1806 \text{ Ma} \pm 27$), or the younger McGregor Volcanics (1740 Ma , Fanning et al, in prep.).

Economic Potential

The thick sequence of carbonates and calcsilicates within Broad View 1 DDH was seen as a potential target for base metal mineralisation similar to that seen at Menninie Dam (Higgins and Helsten, 1986). High Zn values have also been found in similar calcsilicates within the Hutchison Group within the Campoona Syncline, to the south of Broad View 1, by Billiton Aust. (Weeden, 1982). The potential for mineralisation was enhanced by recognition of acid volcanics, possibly within the Hutchison Group metasediments at this locality, which could have been a source of exhalative-style base-metal sulphides. This model was encouraged by the presence of visible pyrite (up to 2% in hand specimen) within both the Bosanquet Formation deformed volcanics and calcsilicates and the underlying Mount Shannan Iron Formation calcsilicates.

However, geochemical analysis of 67 of the samples collected for petrology indicates that the base metal concentrations for both the Mount Shannan Iron Formation and the Bosanquet Formation are typically very low. The best analyses are:

1. Bosanquet Formation

- a. rhyodacites Cu 750ppm Pb <50ppm Zn 790ppm.
- b. calcsilicates Cu 68ppm Pb 255ppm Zn 375ppm.

2. Mount Shannan Iron Formation

Cu 540ppm Pb 195 ppm Zn 200ppm.

Histogram plots for Cu, Pb and Zn values for all samples analysed are shown in Fig. 10.

Although the results for the Broad View 1 DDH are not high, the potential for base metal mineralisation within both the Mount Shannan Iron Formation and the Bosanquet Formation is high, and greater exploration of these horizons along strike should be encouraged.

GEOPHYSICS

Natural gamma, neutron, bulk density and resistivity downhole geophysical logs were compiled for Broad View 1 upon completion of drilling and prior to removal of steel casing. Magnetic susceptibility was measured on the drillcore using a hand-held susceptibility meter. Detailed logs are shown in Figs 11 and 12. All logs show anomalies at 139 and 315 metres, related to variations in steel casings within the hole.

Neutron, Gamma and Bulk Density Logs.

These logs show some broad correlations with lithology. The natural gamma and the bulk density logs both show a decrease in the background level from the transition of the Bosanquet Formation deformed volcanics to the Mount Shannan Iron Formation metasediments.

The neutron log typically shows anomalous highs for the minor calcsilicate gneiss bands within the Bosanquet Formation, with corresponding anomalous lows in the natural gamma count. However, this is not a 1:1 relationship, as some calcsilicate gneiss bands within the Bosanquet Formation show minor anomalous gamma spikes. The deformed rhyodacites show some variability of both neutron and gamma logs, possibly related to variability in the fabric intensity and associated mineralogy. Quartz veins within the volcanics at 66 m and 91 m show anomalous low values

for neutron and gamma counts. The megacrystic rhyodacites near the base of the Bosanquet Formation have slightly higher background neutron levels than the more highly-deformed volcanics.

Within the Mount Shannan Iron Formation, slight anomalous highs in the gamma count correspond to magnetite+amphibole-rich calcsilicate gneiss layers at 450.5 and 464.5 m. The magnetite-rich lithologies show no 1:1 relationship with the bulk density log, reflecting the highly-variable nature of the lithologies which contain magnetite.

Resistivity

Both 16 in. and 64 in. resistivity logs were compiled below the steel casing (from 317m to 490 m).

Within the Bosanquet Formation, the resistivity shows a slight dip in background values associated with fine-grained quartz+biotite+feldspar schists within the deformed volcanics, and a slight rise in background values for the more intensely-deformed volcanics. A marked drop in resistivity at the contacts between the rhyodacite and a calcsilicate gneiss layer (345-351 m) suggests an accumulation of conductive minerals along the contacts. The interlayered calcsilicates typically have slightly lower background levels to the rhyodacite. An anomalous zone of low resistivity from 374-375 m is related to a fracture zone in the rhyodacite which most likely allowed the introduction of conductive fluids.

The Mount Shannan Iron Formation is characterised by markedly lower background values of resistivity than the Bosanquet Formation. The contact between the two units at 408 m, is marked by a sudden drop in resistivity at 409.5 m.

Anomalous low values within the iron formation are correlated on a 1:1 level with magnetite-rich layers within the banded calcsilicates; at 418, 455, 457 and 466 m. The massive, poorly-banded calcsilicate gneiss is marked by an increase in resistivity, reflecting the observed low magnetite content.

Magnetic Susceptibility

Magnetic susceptibility was measured from the drillcore with a hand-held susceptibility meter, as no susceptibility tool was available for downhole logging. The magnetic susceptibility of the core is widely variable, due to variable magnetite content in the various lithologies.

Deformed rhyodacites of the Bosanquet Formation have a low susceptibility, in the range of $20-100 \times 10^{-5}$ SI, with minor increases within the interlayered calcsilicate gneisses (up to 200×10^{-5} SI). There is a very slight increase in magnetic susceptibility from the 'top' to the 'base' of the volcanic sequence.

The calcsilicates of the Mount Shannan Iron Formation have much higher values of magnetic susceptibility, reflecting the high magnetite abundance within the metasediments. The values range from 200 to $80\,000 \times 10^{-5}$ SI. The low values for the calcsilicates are typically within the streaky-laminated biotite+calcite schists and the massive calcsilicate gneisses. The well-banded, amphibole-rich calcsilicate gneisses and the magnetite+quartz+grunerite gneisses typically have high values. The highest values for the magnetite-rich horizons occur at 410.2-410.8m, 491.2-492.1m and 535-538m.

SUMMARY AND STRATIGRAPHIC IMPLICATIONS

Summary

The Broad View 1 DDH intersected 552 m of Early Proterozoic metasediments and metavolcanics. The sequence has been divided on detailed logging and petrographic evidence into two units;

- a) a sequence of metasedimentary calcsilicate and quartzofeldspathic schists and gneisses, including magnetite-rich iron formation, and
- b) an 'overlying' sequence of weakly-deformed to mylonitic, metamorphosed porphyritic rhyodacites with minor, intercalated metasedimentary calcsilicates.

The metasedimentary sequence has been correlated with the Mount Shannan Iron Formation of the Hutchison Group. The metavolcanics have been defined as a new unit; the Bosanquet Formation (Rankin and Flint, in prep). Both formations have been affected by the D_2 and possibly D_3 deformation events of the Kimban Orogeny.

Trace-element and whole-rock silicate geochemical analysis on selected samples indicate that the Bosanquet Formation has a different geochemistry to the Myola Volcanics, their temporal equivalents in the Peake and Denison Inlier (Tidnamurkana Volcanics), and the McGregor Volcanics. Base metal values for both the Mount Shannan Iron Formation and the Bosanquet Formation are very low.

Stratigraphic Implications

The stratigraphic position of the Bosanquet Formation is equivocal with the unit being possibly older, synchronous or even younger than the Mount Shannan Iron Formation. Drillcore around the critical depth at 407.8 m is broken, but the boundary appears relatively sharp. The zone corresponds to a discordance in foliation orientation and significant water loss during drilling suggests at least some discontinuity.

Petrographic evidence of folding and mylonitisation of the Bosanquet Formation indicate that the volcanics predate late stages of the Kimban Orogeny. This is supported by the metamorphic grade in the calcareous metasediments interbedded with the volcanics. Coarse-grained, pale diopside is ubiquitous in exposed conglomeratic calcsilicates, while in the drillcore diopside and hornblende are both present.

Volcanics within the Bosanquet Formation are geochemically dissimilar to other known Early Proterozoic volcanic suites from the eastern Gawler Craton, including the Myola and McGregor Volcanics. Neither of these suites is known to have associated carbonate sedimentation, however both suites are really very restricted and present exposures may not totally reflect past rock types and associations. Thus, volcanics and metasediments of the Bosanquet Formation may equate with either the Myola or McGregor Volcanics.

Conversely, evidence of contemporaneous carbonate-rich sediments (broadly similar to those of the Mount Shannan Iron Formation) during volcanism suggests the Bosanquet Formation may represent a localised volcanic/volcaniclastic facies within the Hutchison Group. No acid volcanics have previously been recognised within the Hutchison Group, so the proven presence of acid volcanism synchronous with deposition of the Mount Shannan Iron Formation has important implications for both the tectonic history and economic potential of the region. Therefore, the Bosanquet Formation rhyodacites are currently being dated using U/Pb zircon geochronology to resolve this stratigraphic problem.

Although the base-metal values for the sequence in Broad View 1 are very low, the association of acid volcanics with carbonate-rich sediments is an encouraging target for base metal mineralisation. Investigation of the economic potential of this sequence both along strike and in the Cainozoic-veneered environs should therefore be encouraged.

LEIGH R. RANKIN

RICHARD B. FLINT

REFERENCES

- Duncan, N., 1976. Exploration Licence No. 218 "Mount Messenger", S.A., relinquishment report. S. Aust. Dept. Mines and Energy, Open File Env., 2732 (unpublished).
- Fanning, C.M., Flint, R.B., Parker, A.J., Ludwig, K.R. and Blissett, A.H. Proterozoic tectonic evolution of the Gawler Craton, South Australia (in prep.).
- Flint, R.B. and Rankin, L.R., in prep. KIMBA map sheet, Geological Atlas of South Australia, 1:250 000 series. Geological Survey of South Australia.
- Floyd, P.A. and Winchester, J.A., 1978. Identification and discrimination of altered and metamorphosed volcanic rocks using immobile elements. Chem. Geol., 21:291-306.
- Higgins, M.L. and Hellsten, K.J., 1986. The Menninnie Dam lead-zinc-silver prospect, South Australia. Abstr. G.S.A. Eighth Aust. Geol. Conv., Adelaide, S.A.
- Parker, A.J., 1983. WHYALLA map sheet, Geological Atlas of South Australia, 1:250 000 series. Geological Survey South Australia.
- Parker, A.J. and Lemon, N.M. 1982. Reconstruction of the Early Proterozoic stratigraphy of the Gawler Craton, South Australia. J. Geol. Soc. Aust., 29:221-238.
- Rankin, L.R. and Flint, R.B., in prep. The Bosanquet Formation of the Gawler Craton. QGN.
- Weeden, R.J., 1982. Exploration Licence No. 877 "Cleve West", S.A., progress report. S. Aust. Dept. Mines and Energy, Open File Env., 3573 (unpublished).

APPENDIX I

THIN SECTION DESCRIPTIONS

6131 RS 66

TS 47917

Depth: 45.70 m

Name: Mylonitic rhyodacite

Hand Specimen:

Fine- to coarse-grained quartz+feldspar+biotite mylonite. The intense foliation anastomoses around abundant quartz and feldspar megacrysts.

Thin Section:

Fine- to coarse-grained, granoblastic-elongate to anastomosing, inequigranular texture. The specimen consists of quartz and microcline megacrysts within a weakly anastomosing matrix of quartz+feldspar+biotite.

Quartz megacrysts have typically suffered dynamic recrystallisation to produce elongate aggregates with lobate internal grain boundaries and intense deformation-band development. Feldspar megacrysts are typically intensely fractured, with recrystallisation of quartz+feldspar+biotite along the fractures. An intense foliation is defined by the preferred-dimensional orientation of quartz/feldspar megacrysts and biotite.

The specimen is a recrystallised porphyritic rhyodacite, with a mylonitic foliation.

6131 RS67

TS 47918

Depth: 49.58 m.

Name: Mylonitic rhyodacite

Hand Specimen:

Fine- to medium-grained, well-foliated quartz+feldspar+biotite mylonite. The foliation anastomoses around abundant attenuated quartz and feldspar megacrysts.

Thin Section:

Fine- to medium-grained, granoblastic-elongate to anastomosing texture. The specimen consists of abundant quartz and microcline megacrysts within an anastomosing matrix of quartz+feldspar+biotite+muscovite.

Quartz megacrysts have typically undergone dynamic recrystallisation, resulting in elongate aggregates of grains with lobate grain boundaries and intense deformation-band and subgrain development. Feldspar megacrysts are fractured, with recrystallisation along the fractures. The matrix grains exhibit undulose extinction.

Late-stage, post-tectonic muscovite has overgrown and partially replaced biotite in the matrix. The specimen is a recrystallised porphyritic rhyodacite with an intense mylonitic fabric defined by the preferred-dimensional orientation of biotite and quartz+feldspar megacrysts.

6131 RS 68

TS 47919

Depth: 50.85 m

Name: Mylonitic rhyodacite

Hand Specimen:

Fine- to medium-grained, granoblastic-elongate to anastomosing, inequigranular texture. The specimen consists of quartz and microcline megacrysts within a weakly anastomosing matrix of fine-grained quartz+microcline+biotite+plagioclase.

Thin Section:

The quartz megacrysts vary from subequant grains, most likely relic phenocrysts, with intense deformation-band development, to aggregates of dynamically-recrystallised grains, with lobate grain boundaries and intense subgrain development. Several quartz megacrysts have a network texture of very fine-grained sericite along internal grain boundaries. Quartz and feldspar grains within the matrix typically exhibit only weak internal strain features, including undulose extinction.

The specimen is a quartz+feldspar+biotite mylonite, most likely developed in a porphyritic rhyodacite. An intense mylonitic foliation is defined by the preferred dimensional orientation of quartz megacrysts, biotite and feldspar+quartz aggregates.

6131 RS69

TS 48238

Depth: 111.43 m

Name: Mylonitic rhyodacite

Hand Specimen:

Fine- to coarse-grained, grey, megacrystic mylonite. Coarse-grained feldspar megacrysts lie within a fine-grained matrix of quartz+feldspar+biotite.

Thin Section:

Fine- to coarse-grained, anastomosing, inequigranular texture. Coarse-grained microcline megacrysts and medium-grained quartz aggregates lie within a fine-grained matrix of quartz+feldspar+biotite. A moderate-intensity mylonitic foliation is defined by the preferred dimensional orientation of biotite. The feldspar megacrysts are typically fractured, with infill of the fractures by quartz+feldspar. Several "megacrysts" consist of fine-grained quartz+feldspar aggregates. Quartz typically exhibits lobate grain boundaries and moderate deformation-banding. Minor epidote occurs in biotite-rich zones.

The original lithology was most likely a porphyritic rhyodacite which has undergone dynamic recrystallisation during deformation/metamorphism.

6131 RS 70

TS 48239

Depth: 112.9 m

Name: Calcsilicate gneiss

Hand Specimen:

Medium-grained, intensely-foliated quartz+feldspar+biotite+calcite gneiss. The foliation is weakly anastomosing.

Thin Section:

Fine- to medium-grained, granoblastic to granoblastic-elongate, inequigranular texture. The specimen has a fine compositional layering (<3-4mm), with bands of fine-grained biotite+quartz+plagioclase alternating with bands of medium-grained, green, poikiloblastic hornblende+calcite+quartz+microcline. Coarse-grained, polycrystalline microcline and quartz megacrysts are rare within the biotite-rich layers. Quartz grains in the megacrysts have lobate grain boundaries and minor deformation-band development.

TS 48240

6131 RS 71

Depth: 114.4m.

Name: Quartz+feldspar+hornblende+biotite+calcite gneiss.

Hand Specimen:

Fine- to medium-grained quartz+feldspar+biotite+calcite gneiss. A moderate gneissic foliation is parallel to a weak compositional banding.

Thin Section:

Fine- to medium-grained, granoblastic to granoblastic-elongate texture. The specimen consists of interlayered narrow bands of fine-grained quartz+biotite+feldspar and medium-grained quartz+feldspar+calcite+hornblende+biotite.

Quartz and feldspar in the fine-grained layers have curved to lobate grain-boundaries and exhibit moderate subgrain development. Rare, coarse-grained microcline megacrysts exhibit evidence of dynamic recrystallisation around the megacryst boundaries. Coarse-grained, polycrystalline quartz bands associated with the fine-grained layers may represent quartz veins.

The medium-grained layers consist of quartz+feldspar+calcite with curved to lobate grain-boundaries. Quartz and feldspar exhibit weak undulose extinction, with dynamic recrystallisation along grain boundaries of rare megacrysts. Hornblende occurs as ragged poikiloblasts associated with medium-grained biotite. The preferred-dimensional orientation of the biotite and the compositional layering define a gneissic foliation.

Accessory phases include apatite, sphene and opaques. The specimen is a finely-banded metasedimentary calcsilicate gneiss.

6131 RS 72

TS 48241

Depth : 127.9 m

Name: Quartz+feldspar+biotite+muscovite blastomylonite.

Hand Specimen:

Fine- to medium-grained, quartz+feldspar+biotite mylonite. An intense mylonitic foliation anastomoses around "clasts" of megacrystic gneiss. The specimen contains minor pyrite.

Thin Section:

Fine- to medium-grained, granoblastic-elongate, inequigranular texture. The specimen consists of fine- to medium-grained quartz+feldspar+biotite+muscovite, with a foliation defined by the preferred-dimensional orientation of the micas. Muscovite appears to be replacing biotite. Abundant coarse-grained microcline megacrysts have undergone moderate to intense dynamic recrystallisation, producing rims and aggregates of fine grains with weak undulose extinction. Polycrystalline quartz aggregates exhibit lobate to serrate grain boundaries and minor deformation-band development.

The specimen contains minor isoclinal folds, with the micas defining an axial-planar foliation. Hinge zones of the folds contain abundant medium-grained, platy biotite and minor magnetite+pyrite. The specimen is most likely a metamorphosed arkosic sediment, with a blastomylonitic to mylonitic foliation.

6131 RS 73

TS 48242

Depth: 134.5m

Name: Quartz+feldspar+mica mylonite.

Hand Specimen:

Medium-grained quartz+feldspar+mica mylonite. An intense mylonitic foliation, weakly anastomosing, is defined by layers of mica and intensely-attenuated quartz/feldspar megacrysts.

Thin Section:

Fine- to medium-grained, granoblastic-elongate to anastomosing, inequigranular texture. The specimen consists of medium- to coarse-grained microcline megacrysts and polycrystalline quartz aggregates within an anastomosing matrix of fine- to medium-grained quartz+feldspar+biotite+muscovite (\pm chlorite).

The microcline megacrysts exhibit partial recrystallisation to fine-grained mosaics with attenuated tails of quartz+feldspar+mica. Polycrystalline quartz aggregates exhibit deformation-band and subgrain development plus dynamic recrystallisation along aggregate boundaries and attenuated tails. The matrix consists of fine-grained biotite+muscovite (\pm chlorite) and thin trails of recrystallised quartz+feldspar. Quartz in the matrix typically exhibits undulose extinction and lobate grain boundaries. Minor fine-grained opaques are intergrown with biotite. Muscovite/chlorite has partially replaced biotite. The specimen has a mylonitic foliation, defined by the preferred dimensional orientation of micas and elongate megacrysts.

6131 RS 74

TS 48243

Depth: 188.95 m

Name: Quartz+feldspar+diopside gneiss.

Hand Specimen:

Medium-grained quartz+feldspar+diopside gneiss, with a moderately-contorted compositional layering.

Thin Section:

Fine- to medium-grained, granoblastic, inequigranular texture. The specimen consists of intergrown, medium-grained diopside+quartz+microcline, with fine-grained calcite. Grain boundaries are typically curved to lobate. Minor microcline megacrysts have fine-grained recrystallised rims. The diopside has been partially replaced by actinolitic hornblende associated with calcite+quartz-filled veins.

A weak gneissic foliation is defined by compositional layering and a weak preferred-dimensional orientation of diopside. The specimen is a metasedimentary calcsilicate gneiss.

6131 RS 75

TS 48244

Depth: 220.2 m

Name: Protomylonitic rhyodacite (?)

Hand Specimen:

Fine- to medium-grained, grey, quartz+feldspar+biotite gneiss, with abundant quartz and feldspar megacrysts. A moderate foliation is parallel to layering and defined by grain size variations of the megacrysts.

Thin Section:

Fine- to coarse-grained, granoblastic-elongate to anastomosing, inequigranular texture. The specimen consists of medium- to coarse-grained microcline and quartz megacrysts within a weakly anastomosing matrix of fine-grained quartz+feldspar+biotite+muscovite.

The feldspar megacrysts exhibit fracturing oblique to the foliation, with infill of recrystallised quartz+feldspar. Quartz megacrysts exhibit intense dynamic recrystallisation to polycrystalline aggregates with lobate grain boundaries and moderate development of deformation banding. The megacrysts typically have attenuated tails of fine, recrystallised quartz+feldspar+biotite.

The matrix consists of fine- to medium-grained biotite+muscovite+quartz+feldspar. The foliation is defined by the preferred-dimensional orientation of micas and megacrysts. The specimen is most likely a recrystallised rhyodacite, with an imposed protomylonitic fabric.

6131 RS 76

TS 48245

Depth: 220.7 m

Name: Blastomylonitic rhyodacite

Hand Specimen:

Medium- to coarse-grained, grey, quartz+feldspar+biotite gneiss, with abundant bluish quartz megacrysts.

Thin Section:

Fine- to coarse-grained, anastomosing, inequigranular texture. The specimen consists of medium- to coarse-grained microcline and quartz megacrysts within an anastomosing matrix of fine-grained quartz+feldspar+biotite+muscovite. The feldspar megacrysts exhibit intense fracturing and partial recrystallisation. Quartz megacrysts typically exhibit well-developed deformation banding and partial recrystallisation to produce polycrystalline aggregates with lobate internal grain boundaries.

The preferred-dimensional orientation of biotite and muscovite in the matrix define an anastomosing foliation. Minor post-foliation muscovite has grown oblique to the foliation (approx. 15-40°). The specimen is most likely a deformed phenocrystic rhyodacite, with an imposed mylonitic fabric.

6131 RS 77

TS 48246

Depth: 291.5 m

Name: Quartz+feldspar gneiss.

Hand Specimen:

Medium-grained, well-foliated quartz+feldspar+biotite gneiss. A moderate gneissic foliation is parallel to a weak compositional layering.

Thin Section:

Fine-grained, granoblastic, equigranular texture. The specimen consists predominantly of granoblastic quartz, with minor microcline (sericitised) and biotite. A weak foliation is defined by the preferred-dimensional orientation of biotite. The quartz grains exhibit curved to weakly-lobate grain boundaries plus weak undulose extinction and deformation-band development.

Minor medium-grained quartz megacrysts have cores exhibiting deformation banding and rims of relatively strain-free recrystallised grains. The specimen may be either a recrystallised rhyodacite or an arkosic metasediment.

6131 RS 78

TS 48247

Depth: 303.2 m

Name: Calcsilicate gneiss

Hand Specimen:

Fine- to medium-grained, grey-green, diopside+amphibole-bearing calcsilicate gneiss. A moderate gneissic foliation is parallel to a weak compositional layering.

Thin Section:

Fine- to medium-grained, granoblastic-elongate, inequigranular texture. The specimen consists of decussate to weakly-oriented aggregates of poikiloblastic, pale-green actinolite surrounded by a matrix of quartz+feldspar+calcite. Quartz occurs both as fine grains associated with microcline+plagioclase and as layers and medium-grained aggregates with lobate grain boundaries and common deformation-band development. Accessory phases include apatite, sphene and magnetite. A weak gneissic foliation is defined by the preferred-dimensional orientation of both amphibole and quartz aggregates, parallel to a weak compositional layering.

6131 RS 79

TS 48248

Depth: 315.5 m.

Name: Quartz+feldspar+biotite gneiss.

Hand Specimen:

Fine- to medium-grained quartz+feldspar+biotite gneiss. The gneissic foliation is defined by both biotite layers and attenuated feldspar megacrysts.

Thin Section:

Fine- to medium-grained, granoblastic to granoblastic-elongate, inequigranular texture. The specimen consists of minor medium- to coarse-grained microcline and quartz megacrysts within a matrix of quartz+microcline+plagioclase+biotite.

Both microcline and quartz megacrysts are lenticular, with intense fracturing and recrystallisation common in the microcline megacrysts. Quartz megacrysts exhibit partial dynamic recrystallisation to produce polycrystalline aggregates with lobate grain boundaries, deformation-banding and subgrain development.

Quartz and feldspar grains within the matrix exhibit undulose extinction and minor subgrain development. Fine- to medium-grained biotite is intergrown with fine-grained opaques. Biotite-free, lenticular aggregates of very fine-grained microcline+quartz in the matrix may represent recrystallised clasts of acid volcanics. The specimen is most likely an arkosic metasediment, with some possible volcanoclastic component.

6131 RS 80

TS 48249

Depth: 318.9 m

Name: Protomylonitic phenocrystic rhyodacite

Hand Specimen:

Fine-grained, grey quartz+feldspar+mica gneiss with abundant coarse-grained, feldspar megacrysts. The megacrysts are elongate, defining a moderate-intensity foliation.

Thin Section:

Fine- to medium-grained, granoblastic-elongate to anastomosing, inequigranular texture. The specimen consists of a matrix of fine-grained quartz+feldspar+biotite weakly anastomosing around lenticular megacrysts and aggregates of microcline and quartz. Microcline megacrysts have undergone partial recrystallisation and sericitisation. Quartz aggregates typically exhibit undulose extinction, lobate grain boundaries and minor subgrain development.

The preferred-dimensional orientation of biotite and elongate megacrysts/aggregates define a weak- to moderate-intensity foliation. Accessory phases include opaques, apatite and epidote.

The specimen is a recrystallised phenocrystic rhyodacite, with an imposed protomylonitic fabric.

6131 RS 81

TS 48250

Depth: 324.7 m.

Name: Quartz+feldspar+biotite gneiss.

Hand Specimen:

Fine-grained, grey, quartz+feldspar+biotite gneiss. The gneissic foliation is parallel to a moderate-intensity compositional layering.

Thin Section:

Fine-grained, granoblastic-elongate, equigranular texture. The specimen consists of fine-grained quartz+feldspar+biotite, with a gneissic foliation defined by the preferred-dimensional orientation of biotite. The quartz and feldspar grains typically exhibit undulose extinction. Rare medium-grained quartz aggregates exhibit lobate grain boundaries and minor subgrain development.

The specimen is a metasedimentary gneiss, the original lithology most likely being a lithic arkose.

6131 RS 82

TS 48251

Depth: 349.0 m

Name: Quartz+biotite+feldspar gneiss

Hand Specimen:

Fine-grained, dark quartz+biotite+feldspar gneiss. A moderate gneissic foliation is parallel to a well-developed compositional layering.

Thin Section:

Fine-grained, granoblastic to granoblastic-elongate, equigranular texture. The specimen consists of a fine-grained mosaic of quartz+plagioclase+biotite, with minor muscovite. A weak foliation is defined by the preferred-dimensional orientation of fine-grained biotite laths.

The specimen is a metasedimentary gneiss, the most likely original lithology being a lithic arkose.

6131 RS 83

TS 48252

Depth: 349.75

Name: Quartz+biotite+feldspar gneiss

Hand Specimen:

Fine-grained, dark grey, quartz+feldspar+biotite gneiss. A weak gneissic foliation is parallel to a weak compositional layering.

Thin Section:

Fine- to medium-grained, granoblastic-elongate, inequigranular texture. The specimen consists of a fine-grained matrix of biotite+quartz+feldspar, with minor medium-grained polycrystalline quartz aggregates. A weak-to moderate-intensity foliation is defined by the preferred-dimensional orientation of biotite and minor quartz ribbons. Accessory phases include minor medium-grained pyrite and magnetite.

The specimen is a fine-grained metasedimentary gneiss. The original lithology was most likely a fine-grained lithic arkose.

6131 RS 84

TS 48253

Depth: 350.5 m.

Name: Biotite+quartz schist.

Hand Specimen:

Fine-grained biotite+quartz schist, with abundant pyrite in thin (<1mm) layers parallel to the schistosity.

Thin Section:

Fine- to medium-grained, granoblastic-elongate, inequigranular texture. The specimen consists of fine-grained quartz+feldspar intergrown with medium-grained laths of biotite (\pm muscovite). A weak foliation is defined by a weak preferred-dimensional orientation of biotite. Pyrite+minor magnetite (?) occur as medium-grained, commonly equant, aggregates intergrown with biotite. Accessory phases include medium-grained calcite, minor chlorite and rare zircons.

The specimen is a semipelitic metasedimentary schist.

6131 RS 85

TS 48254

Depth: 360.7 m.

Name: Recrystallised phenocrystic rhyodacite.

Hand Specimen:

Fine-grained, quartz+feldspar+biotite gneiss (?) with coarse-grained feldspar megacrysts. The foliation is weakly anastomosing.

Thin Section:

Fine- to coarse-grained, anastomosing, inequigranular texture. The specimen consists of coarse-grained, subequant microcline and quartz megacrysts surrounded by a fine-grained matrix of quartz+feldspar+biotite. The quartz megacrysts typically exhibit deformation banding and commonly are recrystallised, forming polycrystalline aggregates. Several quartz megacrysts have embayed grain boundaries, suggesting they are volcanic phenocrysts.

The matrix fabric appears protomylonitic, with evidence of dynamic recrystallisation within both the matrix and along megacryst grain boundaries. The specimen is a recrystallised phenocrystic rhyodacite.

6131 RS 86

TS 48255

Depth: 361.05 m.

Name: Microcline+quartz+mica mylonite.

Hand Specimen:

Fine- to medium-grained quartzofeldspathic mylonite, with a moderate-intensity anastomosing foliation defined by layers of mica.

Thin Section:

Fine- to medium-grained, granoblastic-elongate, inequigranular texture. The specimen consists of quartz and microcline megacrysts within a matrix of fine- to medium-grained quartz+microcline+muscovite+biotite. Biotite typically occurs as large polycrystalline aggregates, associated with minor pyrite.

Fine-grained, polygonal microcline is abundant, both within the matrix and as coronas about quartz and feldspar megacrysts. This texture may be due to metasomatic growth of microcline during influx of a K-rich fluid. A weak mylonitic foliation is defined by compositional banding and a preferred-dimensional orientation of biotite and microcline. Accessory phases include calcite, epidote and apatite.

The specimen is a fine-grained mylonite. The original lithology was most likely a phenocrystic rhyodacite.

6131 RS 87

TS 48256

Depth: 361.23

Name: Quartz+biotite+feldspar gneiss.

Hand Specimen:

Fine-grained, grey, quartz+feldspar+biotite gneiss, with a moderate-intensity gneissic foliation.

Thin Section:

Fine-grained, granoblastic to granoblastic-elongate, equigranular texture. The specimen consists of bands of biotite+minor microcline and quartz interlayered with bands of polygonal quartz+microcline+minor biotite. A gneissic foliation is defined by the compositional layering and a preferred-dimensional orientation of biotite and elongate quartz grains.

Within the biotite-rich layers, elongate trails and veins of pyrite (\pm pyrrhotite?) are associated with minor calcite. The contacts between the biotite and quartz layers are sharp.

The specimen is a fine-grained, finely-layered semipelitic metasedimentary gneiss.

6131 RS 88

TS 48257

Depth: 364.33 m.

Name: Quartz+feldspar+diopside+biotite gneiss.

Hand Specimen:

Fine-grained, well-banded quartz+feldspar+biotite gneiss, with minor diopside.

Thin Section:

Fine- to coarse-grained, granoblastic-elongate, inequigranular texture. The specimen consists of a polygonal mosaic of fine- to medium-grained quartz+feldspar+biotite, with occasional quartz ribbons. Coarse-grained, sieve-textured clinopyroxene grains are common within the quartz-rich layers. Fine-grained, inclusion-rich plagioclase may represent metasomatic feldspar.

The specimen is a well-banded, calcium-rich metasedimentary gneiss.

6131 RS 89

TS 48258

Depth: 377.89 m.

Name: Blastomylonitic phenocrystic rhyodacite

Hand Specimen:

Fine-grained, grey mylonitic gneiss, with a weak foliation anastomosing around coarse-grained, feldspar megacrysts.

Thin Section:

Fine- to coarse-grained, granoblastic-elongate to anastomosing, inequigranular texture. The specimen consists of medium- to coarse-grained quartz and microcline megacrysts within a fine-grained matrix of quartz+feldspar+biotite.

The microcline megacrysts are commonly subequant, fractured and partially recrystallised. Several grains exhibit oblique slip and extension along fractures, with infilling by relatively strain-free, medium-grained quartz. Quartz megacrysts vary from subequant grains with intense undulose extinction, subgrain development and deformation banding, to elongate, recrystallised polycrystalline lenticular aggregates and ribbons. Some weakly-strained grains exhibit embayments, suggesting the quartz megacrysts are volcanic phenocrysts. Medium-grained quartz forms tails to feldspar megacrysts, elongate parallel to the foliation. Zircons are common in this specimen, and are concentrated into narrow bands.

The fine-grained matrix appears to have undergone dynamic recrystallisation, with ubiquitous lobate grain-boundaries and subgrain development. The specimen is a dynamically recrystallised porphyritic rhyodacite, with an imposed blastomylonitic fabric.

6131 RS 90

TS 48259

Depth: 406.8 m

Name: Protomylonitic phenocrystic rhyodacite

Hand Specimen:

Fine-grained, grey schist, with a weak schistosity anastomosing around coarse-grained feldspar megacrysts. The fabric appears weakly mylonitic.

Thin Section:

Fine- to coarse-grained, granoblastic-elongate to anastomosing, inequigranular texture. The specimen consists of coarse-grained, subequant microcline and quartz megacrysts within a fine-grained matrix of quartz+feldspar+biotite.

The microcline megacrysts exhibit lattice kinking and warping, plus recrystallisation along incipient fractures and along grain boundaries. Quartz megacrysts tend to be more elongate, with undulose extinction and deformation-band development. Many quartz grains have undergone partial recrystallisation to produce rims of polygonal, relatively weakly-strained grains.

The matrix grains exhibit undulose extinction and slightly lobate grain-boundaries, suggesting dynamic recrystallisation. A moderate foliation is defined by the preferred dimensional orientation of quartz and biotite. The specimen is a recrystallised phenocrystic rhyodacite, with abundant coarse-grained microcline and quartz phenocrysts. The imposed tectonite fabric is protomylonitic in character.

6131 RS 91

TS 48260

Depth: 409.0 m.

Name: Pyritic quartzite

Hand Specimen:

Fine- to medium-grained, grey-green amphibole schist interlayered with medium-grained quartzite. The quartzite contains abundant pyrite+magnetite.

Thin Section:

Fine- to medium-grained, granoblastic, inequigranular texture. The specimen consists of fine-grained, granoblastic quartz with medium-grained opaques both within veins and as interstitial grains within the matrix. The opaques consist of intergrown and brecciated pyrite+magnetite, and are commonly associated with green chlorite.

The specimen is a metasedimentary quartzite interlayered with amphibole-rich schists. The pyrite+magnetite appears to be post-sedimentary in origin.

6131 RS 92

TS 48261

Depth: 410.2 m.

Name: Banded calcsilicate gneiss.

Hand Specimen:

Fine- to medium-grained, well-foliated metasedimentary gneiss, with layers of quartzite and amphibole+calcite+biotite gneiss. The foliation is parallel to the compositional layering.

Thin Section:

Contact between medium-grained, granoblastic quartzite and amphibole+calcite+biotite-rich calcsilicate gneiss. The contact of the quartzite to bands of calcite+grunerite/hornblende+magnetite is sharp, defined by decussate clusters of grunerite.

There is a second sharp contact between the grunerite-rich layers and a fine-grained biotite+feldspar+epidote gneiss. Medium- to coarse-grained garnet porphyroblasts occur near the contact. A gneissic foliation is defined by both the compositional banding and by the preferred-dimensional orientation of biotite.

6131 RS 93

TS 48262

Depth: 410.3 m

Name: Banded calcsilicate gneiss.

Hand Specimen:

Pale grey-green, fine- to medium-grained banded calcsilicate gneiss. A strong foliation is defined by the preferred-dimensional orientation of biotite+amphiboles.

Thin Section:

Fine- to medium-grained, granoblastic to granoblastic-elongate, inequigranular texture. The specimen consists of interlayered calcite+magnetite+actinolitic hornblende and biotite+actinolitic hornblende+grunerite+magnetite.

The calcite-rich layers have a granoblastic texture, with irregular, inclusion-rich magnetite grains. The magnetite appears intergrown with minor grunerite. Grunerite in the biotite-rich layers appears to be replacing both pale-green hornblende and minor coarse-grained garnet poikiloblasts. The grunerite has an "hourglass" morphology. An intense schistosity is defined in the biotite-rich layers by a strong preferred-dimensional orientation of biotite and grunerite.

6131 RS 94

TS 48263

Depth: 410.8 m.

Name: Quartz+biotite+amphibole+calcite+garnet gneiss.

Hand Specimen:

Medium-grained, amphibole-rich, biotite+quartz+garnet gneiss. The amphibole-rich bands have a decussate texture.

Thin Section:

The specimen is a banded, metasedimentary calcsilicate gneiss, with bands of biotite+quartz+garnet, calcite+magnetite+grunerite/hornblende and quartz+grunerite. The biotite-rich band has an intense schistosity, defined by the preferred-dimensional orientation of biotite. The garnet poikiloblasts are coarse-grained and contain inclusions of grunerite. Within the calcite-rich bands, blue-green hornblende is intergrown with grunerite.

6131 RS 95

Depth: 415.9 m.

Name: Calcsilicate gneiss.

Hand Specimen:

Fine- to medium-grained, dark grey-green amphibole+calcite+magnetite gneiss. A moderate foliation is parallel to a weak compositional layering.

Thin Section:

Fine- to medium-grained, granoblastic to granoblastic-elongate, inequigranular texture. The specimen consists of irregular intergrowths of fine- to medium-grained, blue-green hornblende, biotite and chlorite. Associated with the hornblende is medium-grained magnetite and calcite. At the contact with a layer of medium-grained, granoblastic calcite, chlorite+hornblende has partially replaced medium-grained diopside.

The specimen is a magnetite-rich metasedimentary gneiss. The original lithology was most likely a mixed pelitic+carbonate sedimentary iron formation.

6131 RS 96

TS 48265

Depth: 416.1 m.

Name: Quartz+magnetite gneiss.

Hand Specimen:

Fine-grained, grey quartz+magnetite gneiss, with a moderate foliation parallel to a weak compositional layering.

Thin Section:

Fine- to medium-grained, granoblastic-elongate, inequigranular texture. The specimen consists of medium-grained quartz+fine-grained magnetite, with a weak gneissic foliation axial-planar to tight, angular folds. The foliation is defined by the preferred-dimensional orientation of both quartz and opaques. Quartz ribbons subparallel to the axial-planes of the folds may represent deformed quartz-veins.

Medium-grained grunerite is aligned parallel to the axial-planar fabric. Chlorite has partially replaced grunerite. The specimen is a metasedimentary quartz+magnetite gneiss. The original lithology was most likely a banded iron formation.

6131 RS 97

TS 48266

Depth: 417.8 m.

Name: Diopside+magnetite+quartz gneiss.

Hand Specimen:

Fine- to medium-grained, grey-green amphibole+magnetite+quartz gneiss. Contains tight to isoclinal folds.

Thin Section:

Fine- to coarse-grained, granoblastic, inequigranular texture. The specimen consists of interlayered quartzite and diopside+magnetite+garnet+chlorite gneiss. Pyrite is associated with magnetite. Grunerite is typically associated with the quartz-rich layers. The compositional layering is folded by tight, subangular, hinge-thickened folds. Accessory phases include apatite+calcite.

The specimen is a diopside+magnetite+quartz gneiss, and represents a metamorphosed iron formation.

6131 RS 98

TS 48267

Depth: 419.2 m.

Name: Garnet+grunerite+biotite schist.

Hand Specimen:

Medium-grained biotite+amphibole+quartz schist, with boudinaged layers of coarse-grained garnet.

Thin Section:

Medium- to coarse-grained, granoblastic to decussate, inequigranular texture. The specimen consists of coarse-grained, helicitic garnet porphyroblasts within a matrix of platy biotite and prismatic grunerite. The garnet porphyroblasts contain folded inclusion trails of opaques, with minor post-tectonic, inclusion-free rims. The porphyroblasts are subhedral and typically fractured, with infill of the fractures by grunerite.

The inclusion trails are tightly folded, with an axial-planar fabric defined by trails of opaques. The axial-planar fabric is parallel to the principal foliation of the schist, suggesting the garnets grew during the late stage of the foliation-forming event.

The specimen is a metasedimentary, semi-pelitic garnet+grunerite+biotite schist.

6131 RS 99

TS 48268

Depth: 420.9 m.

Name: Quartz+magnetite+amphibole gneiss.

Hand Specimen:

Fine- to medium-grained quartz+magnetite+amphibole gneiss, with tight to isoclinal folds. Amphibole occurs as decussate clusters.

Thin Section:

Fine-grained, granoblastic, inequigranular texture. The specimen consists of fine-grained quartz+opaques (?magnetite), intergrown in a polygonal mosaic. Quartz typically exhibits undulose extinction. The opaques also occur as fine-grained inclusions within poikiloblastic blue-green hornblende and grunerite.

The specimen is intensely folded, with a weak axial-planar fabric defined by elongate trails of opaques in the thickened hinges of isoclinal folds.

A quartz+chlorite-filled vein perpendicular to the fold axes contains medium-grained chlorite grains that exhibit intense undulose extinction and conjugate kinking. This suggests that the vein formed during the last stages of folding, with minor compression of the vein parallel to its length.

The specimen is a quartz+magnetite + amphibole gneiss, representing a metamorphosed iron formation.

6131 RS 100

TS 48269

Depth: 423.45 m.

Name: Grunerite+biotite+garnet+quartz schist.

Hand Specimen:

Medium-grained, well-banded amphibole+biotite+quartz schist. Garnet porphyroblasts are common within amphibole-rich layers.

Thin Section:

Fine- to coarse-grained, granoblastic-elongate to decussate, inequigranular texture. The specimen consists of interlayered grunerite+biotite+quartz schist, and garnet+biotite schist.

Quartz in the grunerite-rich layers occurs as elongate, polycrystalline aggregates and ribbons with lobate internal grain-boundaries and moderate deformation-band development. Grunerite occurs as fine- to medium-grained clusters of prismatic grains intergrown with biotite, chlorite and minor blue-green hornblende.

The contact between the grunerite-rich schist and the biotite-rich schist is gradational. The biotite-rich schist contains coarse-grained, subequant, poikiloblastic garnets within a matrix of decussate biotite. Minor opaques are associated with the garnet. Garnet is occasionally intergrown with grunerite.

Coarse-grained quartz veins parallel to the compositional layering are bordered by medium-grained grunerite oriented perpendicular to the vein length.

6131 RS 101

TS 48270

Depth: 427.6 m.

Name: Biotite+amphibole+garnet schist.

Hand Specimen:

Fine- to medium-grained, grey-green amphibole+garnet schist with minor quartz+calcite layers.

Thin Section:

Fine- to coarse-grained, granoblastic to decussate, inequigranular texture. The specimen consists of interlayered calcite+diopside, quartzite and grunerite/hornblende+biotite+garnet schist.

Garnet occurs as medium- to coarse-grained porphyroblasts within biotite-rich layers. Garnet has been partially replaced by amphibole+opaques. The amphibole is intergrown grunerite + blue-green hornblende. The amphibole-rich layer is in sharp contact with a fine- to medium-grained quartzite layer with quartz grains exhibiting lobate to serrate grain boundaries and intense deformation-band and subgrain development.

The quartz is in contact with a granoblastic calcite-rich layer, containing medium-grained diopside. The diopside has been partially replaced by amphibole (?hornblende). The specimen is a pelitic, metasedimentary biotite+amphibole+garnet schist.

6131 RS 102

TS 48271

Depth: 437.7 m.

Name: Banded calcsilicate gneiss.

Hand Specimen:

Medium-grained, well - banded calcite+amphibole+diopside calcsilicate gneiss. A moderate gneissic foliation is parallel to the compositional layering. Layering in the calcite-rich layers is weakly contorted.

Thin Section:

Medium- to coarse-grained, granoblastic, inequigranular texture. The specimen is a banded calc-silicate gneiss, with layers of medium-grained calcite+grunerite and coarse-grained quartz+diopside (+medium-grained actinolite). The quartz exhibits weakly-lobate grain boundaries and moderate deformation-band development. The diopside grains are poikiloblastic, intergrown with quartz+calcite+muscovite.

6131 RS 103

TS 48272

Depth: 449.8 m.

Name: Banded calcsilicate gneiss.

Hand Specimen:

Fine- to medium-grained banded calcsilicate gneiss with moderately-contorted compositional layering.

Thin Section:

Medium- to coarse-grained granoblastic-elongate to decussate inequigranular texture. The specimen is a banded metasedimentary calcsilicate gneiss, with bands of calcite+biotite, actinolite+calcite+chlorite and diopside+quartz+actinolite.

The calcite+biotite layer contains medium-grained calcite+laths of green-brown biotite partially replaced by chlorite. A weak gneissic foliation is defined by the preferred-dimensional orientation of biotite. The actinolite+calcite layer consists of medium-grained decussate actinolite prisms intergrown with calcite.

The coarse-grained diopside has been partially replaced by actinolite, and is intergrown with coarse-grained calcite.

6131 RS 104

TS 48273

Depth: 450.2 m.

Name: Biotite+quartz+calcite schist.

Hand Specimen:

Fine- to medium-grained biotite+quartz+calcite schist, with minor layers of calcite+diopside. The schistosity is parallel to compositional layering.

Thin Section:

Fine- to medium-grained, granoblastic-elongate, inequigranular texture. The specimen consists of fine-grained biotite+quartz (+minor opaques) with bands of calcite+diopside+actinolite (+minor muscovite).

The calcite-rich layers contain minor equant, medium-grained opaques associated with diopside.

Two generations of biotite are evident. The first generation defines a schistosity parallel to the compositional banding, while the second generation has grown approximately perpendicular to the principal schistosity.

6131 RS 105

TS 48274

Depth: 451.2 m.

Name: Banded calcsilicate gneiss.

Hand Specimen:

Fine- to medium-grained calcsilicate gneiss, with a gneissic foliation parallel to compositional layering.

Thin Section:

Fine- to coarse-grained, granoblastic to granoblastic-elongate, inequigranular texture. The specimen is a banded calcsilicate gneiss, with thin (<3 mm) bands of actinolitic hornblende+opques interlayered with medium-grained bands of calcite+actinolitic hornblende+biotite (+minor garnet and opques). Diopside is also common in the calcite+hornblende-rich layers. Medium-grained layers of quartz exhibit lobate grain boundaries and weak deformation-band development.

A coarse-grained layer of diopside has been boudinaged, with infill of extensional fractures by medium-grained actinolitic hornblende+calcite+quartz.

6131 RS 106

TS 48275

Depth: 451.9 m.

Name: Quartz+magnetite+grunerite gneiss.

Hand Specimen:

Fine- to medium-grained quartz+magnetite+amphibole gneiss. The gneissic foliation is parallel to a moderate compositional layering.

Thin Section:

Fine-grained, granoblastic to granoblastic-elongate, inequigranular texture. The specimen is a finely-banded quartz+amphibole+magnetite gneiss.

Quartz+magnetite are intergrown in a polygonal mosaic, with a gneissic foliation defined by compositional layering and a weak preferred-dimensional orientation of magnetite. Grunerite occurs as thin (<2 mm) layers and elongate, "hourglass" aggregates within the gneiss. The grunerite aggregates vary from prismatic aggregates parallel to the gneissic foliation, to fine-grained granoblastic aggregates intergrown with chlorite. Medium-grained diopside relics are common, exhibiting replacement by grunerite and actinolitic hornblende.

6131 RS 107

TS 48276

Depth: 456.0 m

Name: Calcsilicate gneiss.

Hand Specimen:

Fine- to medium-grained, well-banded calcsilicate gneiss, with abundant decussate amphibole and magnetite.

Thin Section:

Fine- to coarse-grained, granoblastic to decussate, inequigranular texture. The specimen contains the contact between a quartz+magnetite gneiss and a moderately-well-layered calcsilicate+amphibole gneiss.

The quartz+magnetite gneiss consists of medium-grained, granoblastic quartz, with fine-grained inclusions of magnetite. Minor fine-grained grunerite+calcite is common throughout the gneiss. The contact with the calcsilicate gneiss is sharp, defined by a narrow (<3mm) band of grunerite, in turn bordered by a narrow (<2 mm) band of biotite. The grunerite at the contact consists of acicular grains perpendicular to the contact, suggesting possible metasomatic growth.

The calcsilicate gneiss consists of layers of;

1. medium-grained, granoblastic calcite+magnetite+actinolite+diopside.
2. fine-grained, green biotite+medium-grained magnetite.
3. coarse-grained grunerite+blue-green hornblende+garnet+magnetite+calcite.

Grunerite has partially replaced hornblende and garnet. Garnet is typically poikiloblastic, intergrown with calcite+magnetite+biotite+chlorite. Several garnet grains have grown as rims around a relic core of diopside.

6131 RS 108

TS 48277

Depth: 459.75 m.

Name: Banded calcsilicate schist

Hand Specimen:

Fine-grained biotite+calcite schist, with interlayering of biotite-rich and calcite+diopside-rich bands.

Thin Section:

Fine- to medium-grained, granoblastic-elongate, inequigranular texture. The specimen is a finely-banded calcsilicate schist. Compositional banding is defined by alternating layers of calcite+quartz+biotite and calcite+quartz+diopside. Diopside grains are typically intergrown with medium-grained calcite.

The original lithology was most likely a marl, with a considerable pelitic component.

6131 Rs 109

TS 48278

Depth: 463.1 m.

Name: Biotite+garnet+grunerite schist.

Hand Specimen:

Fine- to medium-grained, grey-green biotite+amphibole schist. The schistosity anastomoses around aggregates of calcite.

Thin Section:

The specimen consists of a fine- to medium-grained quartz+amphibole gneiss in contact with a biotite+garnet+amphibole schist. The quartz-rich gneiss consists of granoblastic quartz+medium-grained aggregates of grunerite and minor diopside. Fine-grained magnetite is associated with grunerite. Quartz typically has lobate to serrate grain boundaries and moderate deformation-band development.

The biotite schist contains coarse-grained, fractured, poikiloblastic garnets intergrown with medium-grained biotite (+minor hornblende). The biotite varies from random to a moderate-intensity preferred orientation defining a moderate-intensity schistosity. Biotite near the contact with the quartz+magnetite gneiss contains abundant very-fine-grained zircon, with abundant radiation-damage haloes present. Garnet+biotite has been partially replaced by medium-grained, decussate clusters of grunerite.

The specimen is an interlayered metasedimentary magnetite-quartzite and pelitic schist.

6131 RS110

TS 48279

Depth: 463.4m.

Name: Banded calcsilicate gneiss.

Hand Specimen:

Medium-grained, well-banded calcite+amphibole+garnet+magnetite calcsilicate gneiss. The gneissic foliation anastomoses around large (<3 cm) aggregates of decussate amphibole.

Thin Section:

Fine- to coarse-grained, granoblastic to granoblastic-elongate, inequigranular texture. The specimen is a banded calcsilicate gneiss, with compositional layering approx. 5-10 mm thick. Compositional layering includes:

quartz+garnet+biotite
garnet+biotite+actinolite
actinolite+garnet+calcite+magnetite
calcite+magnetite+chlorite

Garnet typically occurs as coarse-grained anhedral poikiloblasts. Actinolite appears to have partially replaced garnet in the amphibole-rich layers.

The calcite-rich layers contain fine-grained chlorite laths, oriented to define a weak schistosity.

The specimen is a well-banded, metasedimentary, semipelitic, calcsilicate gneiss.

6131 RS 111

TS 48280

Depth: 464.1 m.

Name: Banded calcsilicate gneiss.

Hand Specimen:

Fine- to medium-grained banded calcsilicate gneiss, with abundant green amphibole.

Thin Section:

Medium-grained, granoblastic to decussate, inequigranular texture. The specimen consists of layers of decussate actinolitic hornblende+biotite+opagues, calcite+actinolitic hornblende and quartz+opagues+hornblende. Quartz is granoblastic, with ubiquitous undulose extinction.

The actinolitic hornblende varies from pale to dark green, with partial alteration to chlorite. Minor diopside porphyroblasts within the calcite-rich layers have been partially replaced by amphibole.

6131 RS 112

TS 48281

Depth: 468.75 m.

Name: Diopside+actinolite+biotite+calcite gneiss.

Hand Specimen:

Medium-grained, moderately-well-banded calcsilicate gneiss. Layering is defined by concentrations of calcite+diopside and biotite+amphibole.

Thin Section:

Medium- to coarse-grained, granoblastic to granoblastic-elongate, inequigranular texture. The specimen consists of abundant medium- to coarse-grained diopside poikiloblasts partially replaced by actinolite. Biotite is intergrown with the actinolite. The diopside lies within a matrix of calcite+biotite+actinolite, with minor layers of biotite+quartz. Minor epidote is associated with biotite-rich layers.

6131 RS 113

TS 48282

Depth: 472.65 m.

Name: Calcsilicate gneiss

Hand Specimen:

Medium-grained, poorly-banded calcsilicate gneiss. The gneissic foliation is defined by elongate aggregates of calcite and quartz.

Thin Section:

Medium- to coarse-grained, granoblastic to granoblastic-elongate, inequigranular texture. The specimen is compositionally banded, with medium- to coarse-grained diopside+quartz interlayered with bands of medium-grained calcite+biotite. Diopside occurs only within or on the margin of quartz-rich layers and its contact with the calcite-rich layers.

Diopside poikiloblasts are surrounded and partially replaced by decussate actinolite. Quartz is granoblastic, with straight to lobate grain-boundaries and weak deformation-band development. Calcite-rich layers exhibit a weak gneissic foliation, defined by a weak preferred-dimensional orientation of calcite+fine-grained biotite.

6131 RS 114

TS 48283

Depth: 473.8 m.

Name: Quartz+feldspar+biotite schist.

Hand Specimen:

Fine-grained biotite+quartz+feldspar schist, with a moderate schistosity parallel to a weak compositional banding.

Thin Section:

Fine- to medium-grained, granoblastic-elongate inequigranular texture. The specimen consists of fine-grained quartz+microcline+opaques+biotite, with a moderate schistosity defined by compositional banding and the preferred-dimensional orientation of biotite. Minor fine-grained muscovite has partially overgrown biotite to form a retrograde foliation oblique to the principal layer-parallel schistosity.

Several medium-grained layers of microcline+quartz contain rare hornblende porphyroblasts. Plagioclase is also associated with the quartz-rich layers. The specimen is a semipelitic metasedimentary schist.

6131 RS 115

TS 48284

Depth: 479.65 m.

Name: Calcite+biotite marble.

Hand Specimen:

Fine- to medium-grained, grey-green calcite+biotite+amphibole calcsilicate gneiss. The specimen is tightly folded.

Thin Section:

Medium-grained, granoblastic to decussate, inequigranular texture. The specimen consists of granoblastic calcite and decussate, pale green-brown biotite. The biotite is commonly kinked. Minor fold hinges are defined by thickened layers of biotite, with a weak axial-planar fabric defined by minor, recrystallised and partially chloritised biotite. The biotite has almost completely replaced pale-green hornblende, seen as minor relic grains.

Magnetite occurs both as elongate grains associated with biotite, and as skeletal grains intergrown with calcite and grunerite. The specimen is a biotite-rich marble. The original lithology was most likely a marl.

6131 RS 116

TS 48285

Depth: 482.95 m.

Name: Banded calcsilicate gneiss

Hand Specimen:

Fine- to medium-grained banded calcsilicate gneiss, with layers of amphibole+calcite, quartz+feldspar and biotite. A moderate gneissic foliation is parallel to the layering.

Thin Section:

Fine- to medium-grained, granoblastic to granoblastic-elongate, inequigranular texture. The specimen is a banded calcsilicate gneiss, with compositional layering:

quartz+microcline+diopside

calcite+diopside+hornblende+opaques

biotite+opaques+quartz (+minor hornblende)

The layering is approx. 3mm to 20 mm thick.

Diopside typically occurs as anhedral, ragged composite porphyroblasts, partially replaced by hornblende. Fine-grained sphene is a common accessory phase in the diopside-rich layers. Calcite typically occurs as thin (<3mm) bands, with lobate to serrate grain boundaries.

6131 RS 117

TS 48286

Depth: 484.1 m.

Name: Biotite+calcite+hornblende schist.

Hand Specimen:

Fine- to medium-grained, grey biotite+hornblende+calcite schist. The schistosity is sub-parallel to compositional layering.

Thin Section:

Fine- to medium-grained, granoblastic-elongate, inequigranular texture. The specimen consists of medium-grained biotite laths aligned to define a strong schistosity. Calcite occurs as narrow (<1mm), lenticular aggregates and as individual grains between biotite laths. Fine- to medium-grained opaques (magnetite?) are elongate parallel to the schistosity.

Hornblende occurs as medium-grained poikiloblasts, with abundant inclusions of opaques, and appears to be partially replaced by biotite.

A spaced cleavage occurs in one biotite-rich zone, sub-parallel to the schistosity. The cleavage is defined by finely-recrystallised biotite and trails of opaques. The cleavage is most likely a late-stage deformation partially overprinting the schistosity-forming event. A second, minor, generation of biotite grains overprints the schistosity at a high angle.

6131 RS 118

TS 48 287

Depth: 491. 17 m.

Name: Banded calcsilicate gneiss

Hand Specimen:

Fine- to medium-grained calcite+amphibole gneiss with minor quartzite bands. A weak gneissic foliation is parallel to a moderate compositional layering.

Thin Section:

Fine- to medium-grained, granoblastic to decussate, inequigranular texture. The specimen consists of a medium-grained, granoblastic quartzite, grading into a fine- to medium-grained diopside+amphibole+calcite+quartz+magnetite calcsilicate gneiss.

Within the quartzite are elongate pods of fine- to medium-grained grunerite, some with an "hourglass" morphology. The grunerite is commonly associated with medium-grained pyrite+magnetite. The quartzite grades into a grunerite+actinolite-rich gneiss, with abundant fine- to medium-grained garnet. The amphibole has a granoblastic to decussate texture, and is partially altered to chlorite. Coarse-grained, poikiloblastic diopside is intergrown with calcite and partially replaced by amphibole. Calcite-rich layers contain abundant medium-grained opaques (magnetite+pyrite).

6131 RS 119

TS 48288

Depth: 491.57 m.

Name: Calcsilicate gneiss.

Hand Specimen:

Fine- to medium-grained, grey-green amphibole+biotite+calcite calcsilicate gneiss. Coarse-grained garnet poikiloblasts are common. A gneissic foliation is parallel to the compositional layering.

Thin Section:

Fine- to coarse-grained, granoblastic-elongate, inequigranular texture. The specimen is a finely-layered calcsilicate gneiss, with layering ranging from 0.5 mm to 20 mm. Biotite+actinolite define a foliation parallel to the compositional layering, with partial replacement of biotite+chlorite. Some layers of predominantly actinolite have a granoblastic texture with no preferred-dimensional orientation.

Garnet occurs as coarse-grained poikiloblasts, partially replaced by biotite+actinolite. Coarse-grained, poikiloblastic diopside is intergrown with biotite and has been partially replaced by actinolite. Magnetite occurs as irregular aggregates of fine grains associated with calcite-rich layers. Calcite typically occurs within the biotite+actinolite-rich layers.

6131 RS 120

TS 48289

Depth: 492.1 m.

Name: Diopside+amphibole gneiss.

Hand Specimen:

Medium-grained, grey-green amphibole+diopside gneiss. A gneissic foliation is parallel to a well-developed compositional layering. Minor pyrite is evident.

Thin Section:

Medium- to coarse-grained, granoblastic to granoblastic-elongate, inequigranular texture. The specimen consists of coarse-grained, poikiloblastic diopside surrounded and partially replaced by medium-grained actinolitic hornblende. The amphibole varies from a granoblastic mosaic to zones of recrystallised, slightly coarser grains defining a weak foliation.

Medium-grained calcite occurs both as narrow (<2mm) layers with amphibole, and typically intergrown with diopside. Minor garnet, biotite and chlorite are associated with a layer-parallel, coarse-grained pyrite vein. Fine- to medium-grained pyrite also occurs disseminated throughout the amphibole+diopside-rich layers. A gneissic foliation is defined by both compositional layering and a weak preferred-dimensional orientation of diopside and amphibole.

6131 RS 121

TS 48290

Depth: 492.3 m.

Name: Amphibole+garnet schist

Hand Specimen:

Fine- to medium-grained, well-banded garnet+amphibole+calcite schist. The schistosity is defined by the orientation of amphibole grains, and is parallel to the compositional layering.

Thin Sections:

Fine- to medium-grained, granoblastic to granoblastic-elongate, inequigranular texture. The specimen consists of medium-grained grunerite+blue-green hornblende, with coarse-grained poikiloblasts of garnet.

The hornblende typically occurs as granoblastic-elongate mosaics, with fine-grained magnetite. A weak schistosity is defined by a weak preferred-dimensional orientation of hornblende, and is parallel to the compositional layering. Grunerite occurs as decussate, to weakly-aligned aggregates of prismatic grains, partially replacing garnet. Garnet is intergrown with medium-grained biotite, magnetite and calcite. Quartzite layers consist of fine- to medium-grained, granoblastic quartz, with fine-grained inclusions of diopside. Apatite occurs as an accessory phase.

The specimen is a pelitic metasedimentary schist.

6131 RS 122

TS 48291

Depth: 497.7 m

Name: Calcsilicate gneiss

Hand Specimen:

Medium-grained, dark calcite+biotite+amphibole gneiss. There is a weak foliation parallel to a poorly-developed compositional layering.

Thin Section:

Medium- to coarse-grained, granoblastic, inequigranular texture. The specimen is poorly-banded, with medium-to coarse-grained calcite+biotite surrounding abundant, large aggregates of medium-grained diopside. The diopside is partially replaced by actinolitic hornblende. Biotite is partially replaced by chlorite, and is associated with fine-grained magnetite.

6131 RS 123

TS 48292

Depth: 497.95 m.

Name: Microcline+biotite schist

Hand Specimen:

Fine-grained biotite+quartz+feldspar schist. Rare feldspar augen are elongate parallel to a moderate-intensity schistosity.

Thin Section:

Fine- to medium-grained, granoblastic-elongate, inequigranular texture. The specimen consists of fine-grained, subequant microcline and biotite, plus minor fine-grained quartz, with a weak foliation defined by the preferred-dimensional orientation of biotite. Magnetite is abundant, occurring as fine grains scattered throughout the specimen.

Several large aggregates of medium-grained, partially recrystallised microcline occur. Medium-grained sphene+biotite+calcite are associated with the coarse-grained microcline. The specimen is most likely a semipelitic metasedimentary schist.

6131 RS 124

TS 48293

Depth: 498.55 m.

Name: Quartz+feldspar+biotite+sillimanite schist.

Hand Specimen:

Fine-grained quartz+feldspar+biotite schist. Medium-grained feldspar augen are elongate parallel to the schistosity.

Thin Section:

Fine- to medium-grained, anastomosing, inequigranular texture. The specimen consists of elongate aggregates of microcline+quartz within a very-fine-grained matrix of quartz+feldspar +biotite+muscovite+opaques. Microcline and quartz within the lenticular aggregates have straight to weakly-lobate grain boundaries and undulose extinction. There is a weak foliation at approx. 40° to the principal compositional layering. This foliation is best developed in thin (<1mm) bands of very-fine-grained, acicular sillimanite.

The specimen is a semipelitic metasedimentary schist.

6131 RS 125

TS 48294

Depth: 504.35 m.

Name: Biotite+calcite+diopside schist.

Hand Specimen:

Fine- to medium-grained, grey biotite+calcite schist. An intense schistosity anastomoses around medium-grained lenticular calcite aggregates.

Thin Section:

Medium-grained, granoblastic-elongate to anastomosing, inequigranular texture. The specimen consists of lenticular aggregates and thin (<1mm) layers of calcite+irregular diopside within a matrix of biotite+calcite+epidote. The specimen has an intense schistosity, defined by the preferred-dimensional orientation of biotite.

6131 RS 126

TS 48295

Depth: 521.3 m.

Name: Hornblende+calcite amphibolite.

Hand Specimen:

Fine-grained, weakly-layered hornblende+calcite amphibolite. A moderate foliation is parallel to the compositional layering.

Thin Section:

Fine- to medium-grained, granoblastic-elongate, inequigranular texture. The specimen consists predominantly of intergrown, medium-grained hornblende, plus minor biotite, quartz and abundant, finely-dispersed magnetite. Calcite occurs both as fine to medium grains intergrown with hornblende, and as late-stage, cross-cutting veins.

6131 RS 127

TS 48296

Depth: 528.4 m.

Name: Hornblende+biotite schist.

Hand Specimen:

Fine- to medium-grained amphibole+biotite+quartz schist. The schistosity is parallel to a poorly-defined compositional layering.

Thin Section:

Fine- to coarse-grained, decussate, inequigranular texture. The specimen consists of medium-grained, ragged, prismatic, actinolitic hornblende+biotite, with a weak foliation defined by a weak preferred-dimensional orientation of amphibole. Fine- to medium-grained magnetite is associated with the amphibole, and less abundantly with biotite. Green spinel is commonly associated with the magnetite.

The amphibole+biotite schist grades into a biotite+feldspar+quartz schist, with a matrix of fine-grained, granoblastic quartz+feldspar. The quartz + feldspar-rich schist is in contact with a coarse-grained calcsilicate, containing calcite+quartz+diopside+actinolite. Calcite also occurs within the amphibole schist as thin (<0.5 mm) layers.

The specimen is a layered semipelitic metasedimentary schist.

6131 RS 128

TS 48297

Depth: 535.0 m.

Name: Calcsilicate gneiss.

Hand Specimen:

Fine- to medium-grained, grey-green, calcite+amphibole gneiss. A moderate foliation is parallel to a well-defined compositional layering.

Thin Section:

Medium- to coarse-grained, granoblastic-elongate, inequigranular texture. Anhedral, poikiloblastic diopside, partially replaced by hornblende, is intergrown with microcline+quartz. Biotite-rich layers contain coarser-grained hornblende and lenticular aggregates of quartz. The biotite has a weak preferred-dimensional orientation, defining a weak schistosity parallel to compositional layering.

Coarse (<10 mm) diopside grains intergrown with calcite occurs in one layer with partial replacement by hornblende occurring along the margins of the layer.

6131 RS 129

TS 48298

Depth: 535.0 m.

Name: Magnetite+biotite+amphibole schist.

Hand Specimen:

Fine-grained, dark grey-green schist with bands of biotite, green amphibole and magnetite. A strong schistosity is parallel to the compositional layering.

Thin Section:

Fine- to medium-grained, granoblastic to granoblastic-elongate, inequigranular texture. The specimen consists of layers of:

magnetite+biotite±grunerite.

magnetite+quartz±blue-green hornblende.

calcite+biotite+actinolite.

quartz+biotite+hornblende.

A strong schistosity is defined within the biotite+hornblende layers by the preferred-dimensional orientation of biotite. Within the magnetite-rich layers, biotite has a more random, platy texture. The blue-green hornblende within the magnetite-rich layers is associated with grunerite.

6131 RS 130

TS 48299

Depth: 539.3 m.

Name: Quartz+biotite+magnetite schist.

Hand Specimen:

Fine- to medium-grained, well-banded biotite+magnetite+quartz schist. The schistosity is parallel to the compositional layering.

Thin Section:

Fine- to medium-grained, granoblastic-elongate, inequigranular texture. The specimen consists of fine-grained quartz+biotite+magnetite+minor hornblende, with a strong schistosity defined by both compositional layering and the preferred-dimensional orientation of biotite. Lenticular aggregates of medium-grained calcite are parallel to the compositional layering. Medium-grained, anhedral sphene is associated with the calcite.

This banded quartz+biotite+calcite schist is in gradational contact with a very-fine-grained quartz+magnetite+microcline+amphibole schist. Microcline occurs as elongate, lenticular aggregates parallel to a schistosity defined by the preferred-dimensional orientation of fine-grained, sericite and minor biotite.

6131 RS 131

TS 48300

Depth: 545.5 m.

Name: Marble.

Hand Specimen:

Fine- to medium-grained, grey marble, with minor bands of green amphibole+disseminated fine-grained opaques.

Thin Section:

Fine- to medium-grained, granoblastic, inequigranular texture. The specimen consists predominantly of calcite+opaques (?magnetite), with minor green biotite. The opaques typically occur as granoblastic grains within the calcite matrix, although many grains have a skeletal texture, intergrown with grunerite. The (?)magnetite+grunerite appears to have replaced hypersthene, which occurs as fine-grained relics. The specimen is an impure marble.

6131 RS 132

TS 48301

Depth: 556.25 m.

Name: Biotite+calcite schist/calcsilicate gneiss.

Hand Specimen:

Fine- to medium-grained, well-foliated biotite+calcite schist, in contact with a medium-grained diopside+calcite calcsilicate gneiss. The schistosity anastomoses around lenticular aggregates of calcite.

Thin Section:

Medium- to coarse-grained, granoblastic to anastomosing, inequigranular texture. The specimen consists of a biotite+hornblende+calcite schist in contact with a calcite+diopside+hornblende+calcsilicate gneiss.

The schist consists of lenticular aggregates of coarse-grained calcite surrounded by a matrix of medium-grained biotite+calcite+magnetite. Minor hornblende poikiloblasts are partially replaced by biotite. The calcsilicate gneiss consists of granoblastic diopside intergrown with calcite+quartz+minor feldspar+minor hornblende. Fine-grained magnetite is associated with the hornblende.

6131 RS 133

TS 48302

Depth: 558.25 m.

Name: Biotite+amphibole schist.

Hand Specimen:

Fine- to medium-grained, grey-green, well-foliated biotite+amphibole schist. Minor calcite-rich layers.

Thin Section:

Fine- to medium-grained, granoblastic-elongate, inequigranular texture. The specimen consists of actinolitic hornblende/grunerite(?) +biotite+opagues+minor quartz+felspar, with an intense schistosity defined by the preferred-dimensional orientation of biotite+amphiboles+opagues. A narrow (<5 mm) layer of medium-grained calcite+diopside may represent a layer-parallel vein.

6131 RS 134

TS 48303

Depth: 562.25 m.

Name: Banded calcsilicate schist.

Hand Specimen:

Fine- to medium-grained, banded biotite+calcite schist. Schistosity is well defined and weakly anastomosing.

Thin Section:

Medium-grained, granoblastic-elongate, inequigranular texture. The specimen consists of alternating layers (approx. 3-8 mm thick) of diopside+calcite+quartz+feldspar (+minor biotite+sphene+hornblende), and biotite+opaques+quartz (+minor hornblende).

Calcite grains commonly display curved twins, with minor recrystallisation in the intensely-strained grains. A strong schistosity is defined by both the compositional layering and the preferred-dimensional orientation of biotite. The specimen is a banded calcsilicate schist.

6131 RS 135

TS 48304

Depth: 573.55 m.

Name: Biotite+hornblende+calcite schist.

Hand Specimen:

Fine- to medium-grained, banded biotite + calcite schist. The schistosity weakly anastomoses about fine lenticular aggregates of calcite.

Thin Section:

Medium-grained, granoblastic-elongate, equigranular texture. The specimen consists of interlayered calcite+diopside+hornblende and biotite+hornblende+quartz plagioclase. Calcite occurs predominantly as lenticular aggregates and thin (<3 mm) layers associated with poikiloblastic diopside and sphene. Diopside has been partially replaced by hornblende.

Hornblende in the biotite-rich layers has been partially replaced by biotite and opaques. An intense schistosity is defined both the compositional layering and the preferred-dimensional orientation of biotite and hornblende.

APPENDIX II

PLATES

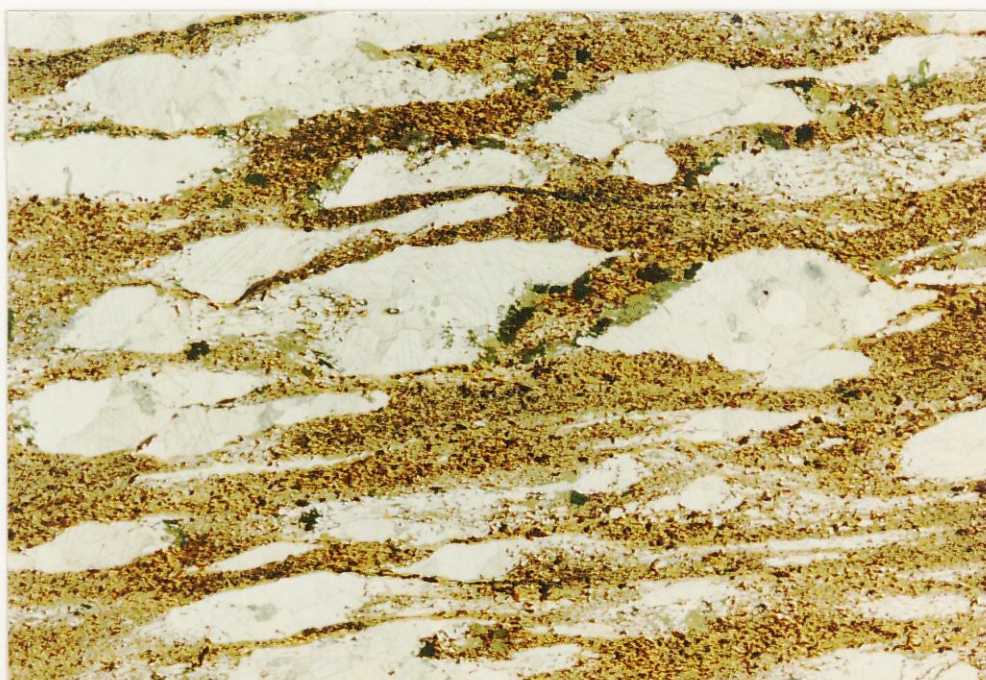


Plate 1. 6131 RS 132, 556.25 m: Mount Shannan Iron Formation. Calcite + biotite + magnetite schist, with lenticular aggregates of calcite. Minor pale-green actinolitic hornblende partially rims some calcite aggregates. Field of view 16 mm x 11 mm. (Plane polarised light)

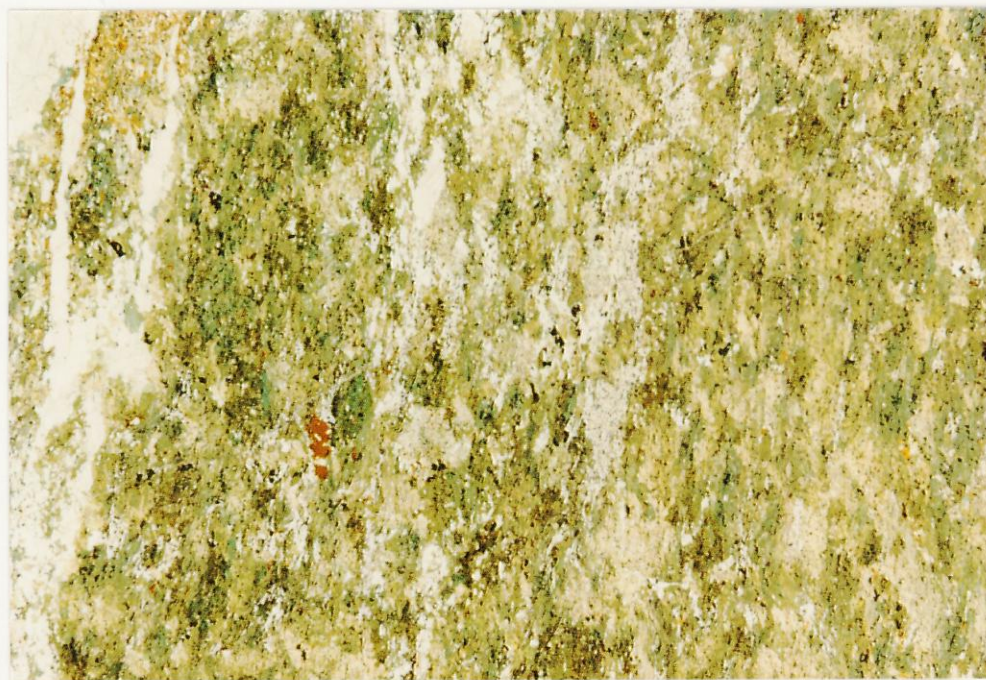


Plate 2. 6131 RS 126, 521.3m: Mount Shannan Iron Formation. Calcite + actinolitic-hornblende schist. Note fine-grained magnetite intergrown with the pale-green actinolitic hornblende. Field of view 16 mm x 11 mm. (Plane polarised light)

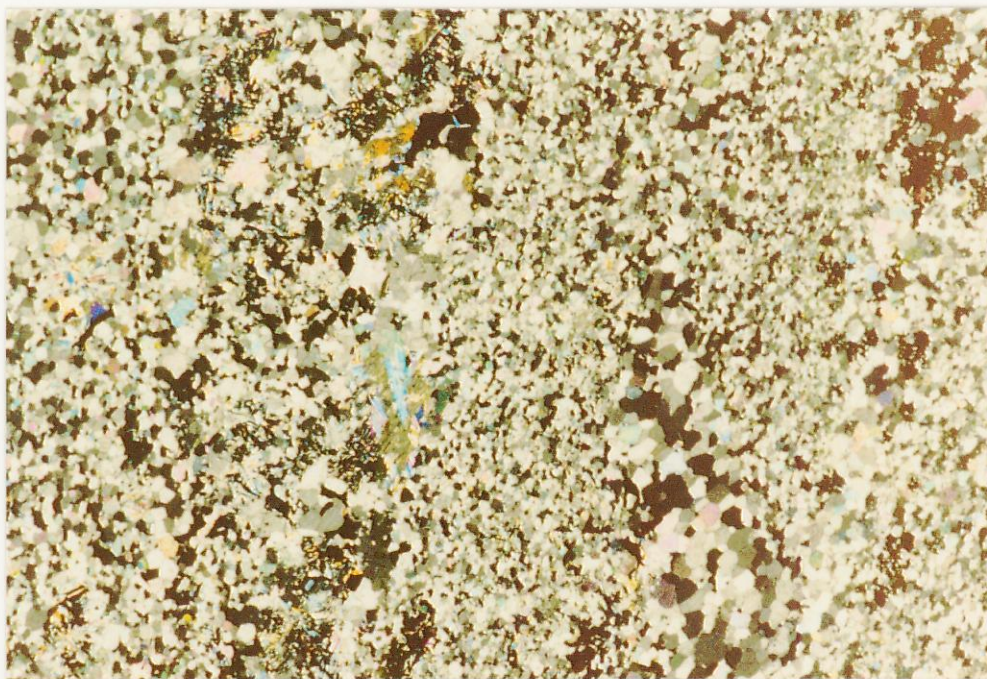


Plate 3. 6131 RS 131, 545.5 m: Mount Shannan Iron Formation. Granoblastic calcite + magnetite + grunerite marble. Note minor skeletal magnetite intergrown with fine-grained grunerite (blue-orange). Field of view 16 mm x 11 mm. (Crossed nicols)



Plate 4. 6131 RS 122, 497.7 m: Mount Shannan Iron Formation. Medium-grained calcite + biotite + diopside gneiss. Note granoblastic texture. Field of view 16 mm x 11 mm. (Crossed nicols)

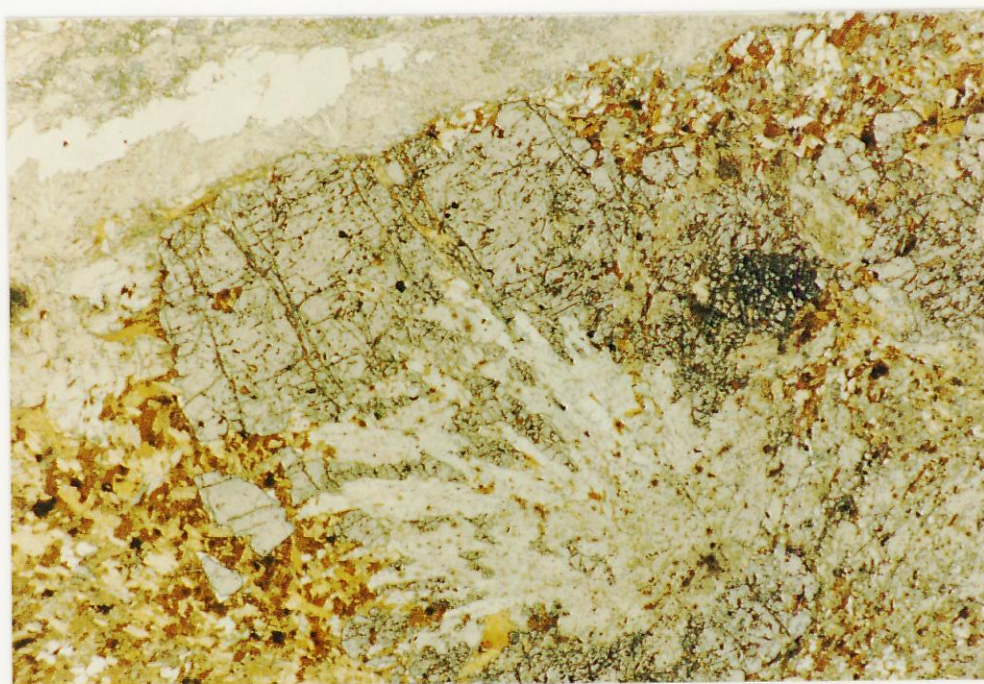


Plate 5. 6131 RS 100, 423.45 m: Mount Shannan Iron Formation. Grunerite + biotite + garnet + quartz schist. Note replacement of garnet by grunerite (colourless). Field of view 4 mm x 2.8 mm. (Plane polarised light)



Plate 6. 6131 RS101, 427.6 m: Mount Shannan Iron Formation. Biotite + amphibole + garnet schist. Note intergrowth of actinolitic hornblende (green) and grunerite (pale fawn). Field of view 16 mm x 11 mm. (Plane polarised light)

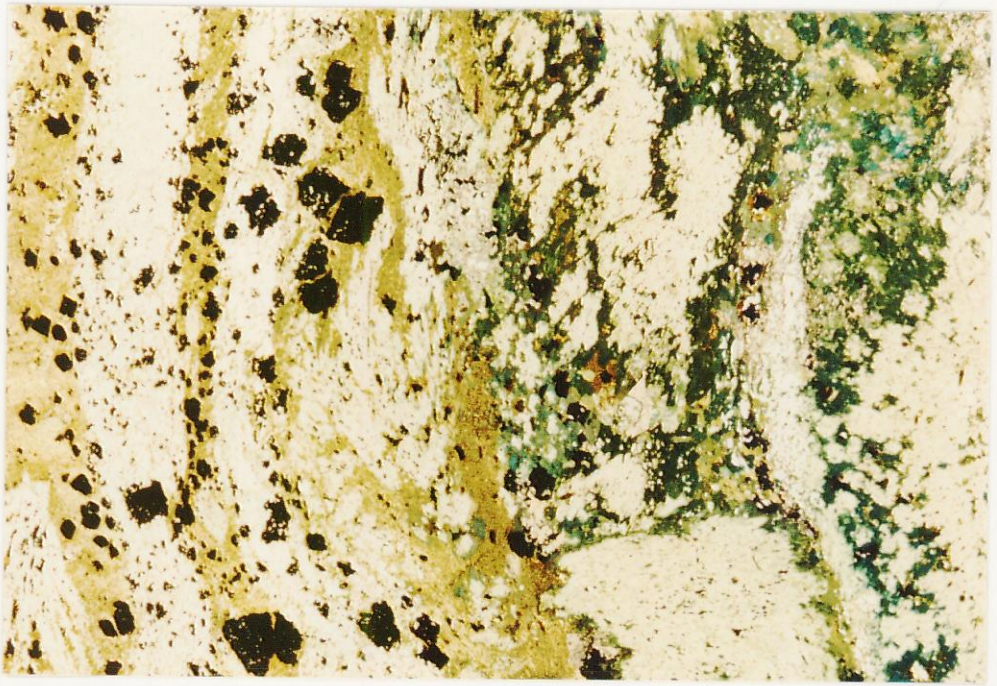


Plate 7. 6131 RS 107, 456.0m: Mount Shannan Iron Formation. Grunerite + actinolitic hornblende + biotite + magnetite gneiss. Field of view 16 mm x 11 mm. (Plane polarised light)



Plate 8. 6131 RS 102, 437.7 m: Mount Shannan Iron Formation. Banded calcsilicate gneiss, with compositional layers of diopside + garnet, quartz, grunerite and calcite + grunerite. The fine-grained grunerite prisms along the contact of the quartz and calcite layers core are oriented perpendicular to the layering. Field of view 16 mm x 11 mm. (Crossed nicols)

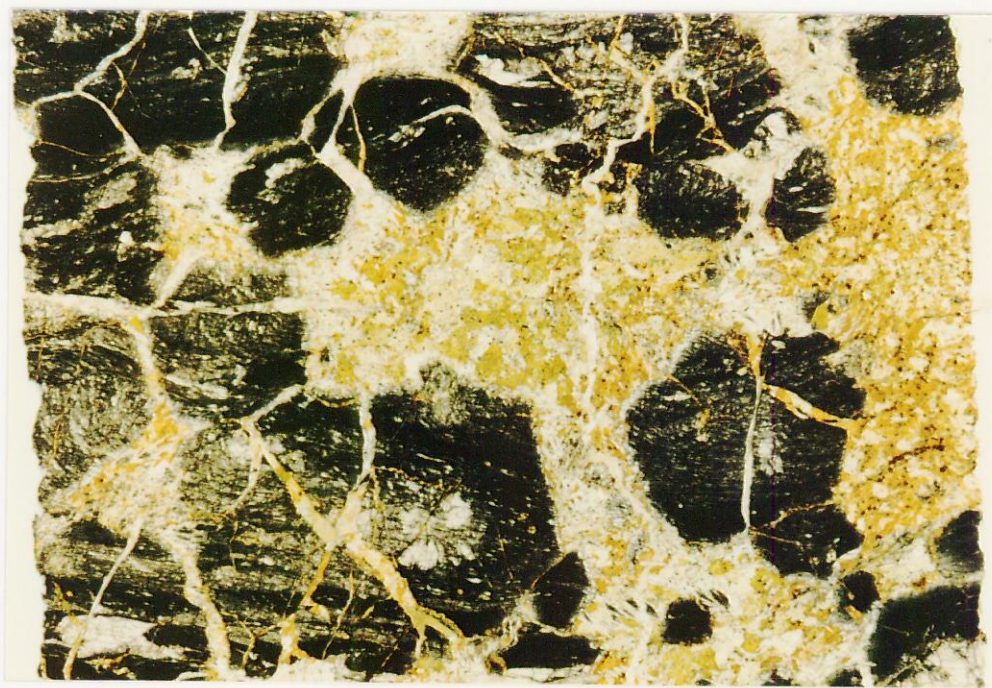


Plate 9. 6131 RS 98, 419.2 m: Mount Shannan Iron Formation. Coarse-grained helicitic garnets within a garnet + grunerite + biotite schist. The garnets have overgrown a folded foliation defined by fine-grained trails of opaques. A weak axial-planar fabric within the garnets is parallel to the mesoscopic S_1 metamorphic foliation. Field of view 16 mm x 11 mm. (Plane polarised light)

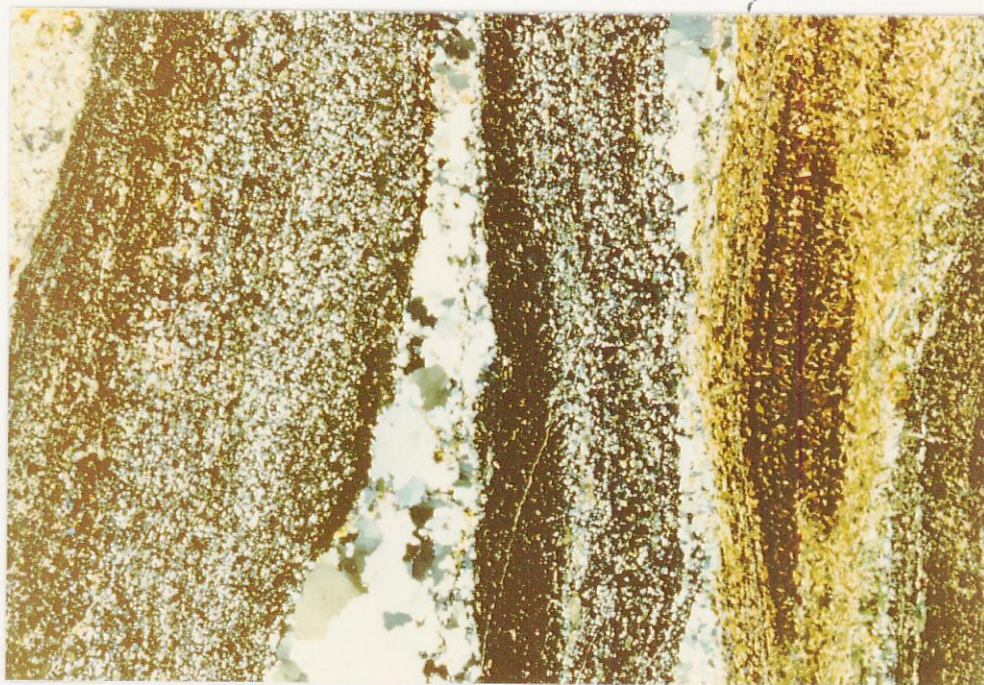


Plate 10. 6131 RS 129, 535.0 m: Mount Shannan Iron Formation. Well-defined compositional layering within a fine- to medium-grained magnetite + quartz + biotite gneiss. Field of view 16 mm x 11 mm. (Plane polarised light)



Plate 11. 6131 RS 92, 410.2 m: Mount Shannan Iron Formation. Contact between magnetite-quartzite and a banded calcsilicate gneiss. Grunerite has grown along the contact as elongate prisms perpendicular to the compositional layering. Field of view 16 mm x 11 mm. (Crossed nicols)

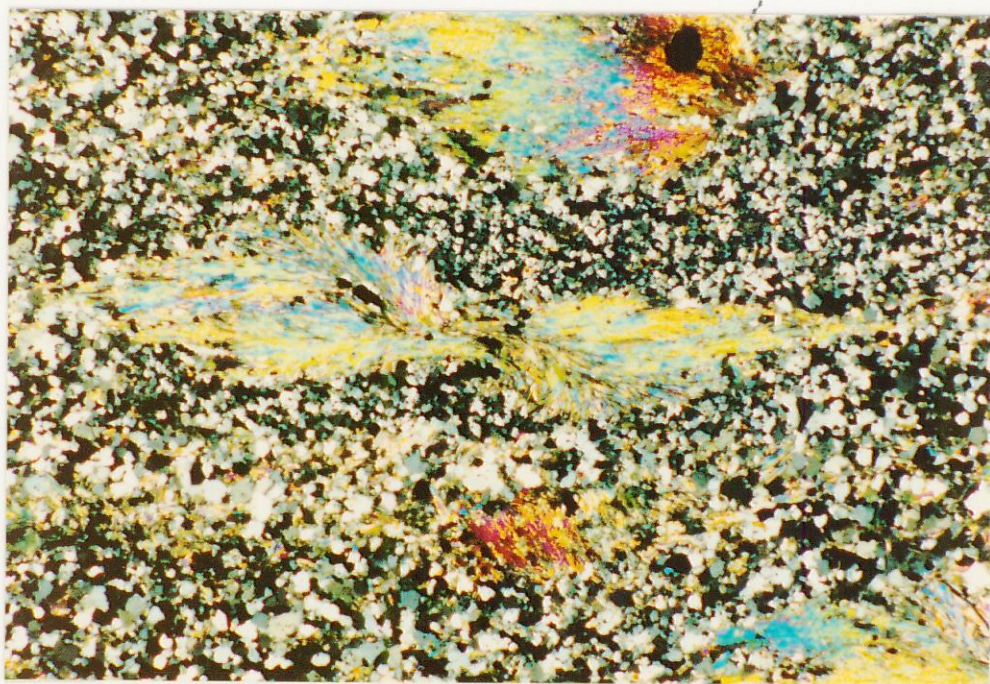


Plate 12. 6131 RS 106, 405.9 m: Mount Shannan Iron Formation. Fine-grained grunerite with "hourglass" morphology within a quartz + magnetite + amphibole gneiss. Field of view 3.5 mm x 2.4 mm. (Crossed nicols)

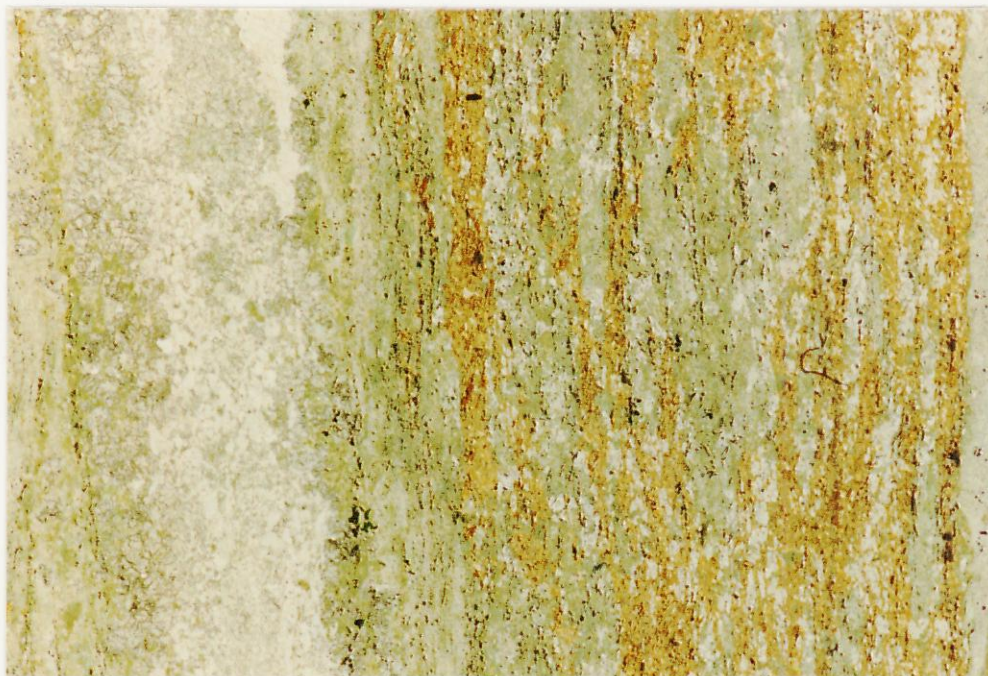


Plate 13. 6131 RS 133, 558.25 m: Mount Shannan Iron Formation. Fine- to medium-grained biotite (brown) + actinolitic hornblende (green) + magnetite schist in contact with a calcite + diopside gneiss (colourless). Note microfolds in amphibole layering, with axial-planar magnetite trails. Field of view 16 mm x 11 mm. (Plane polarised light)

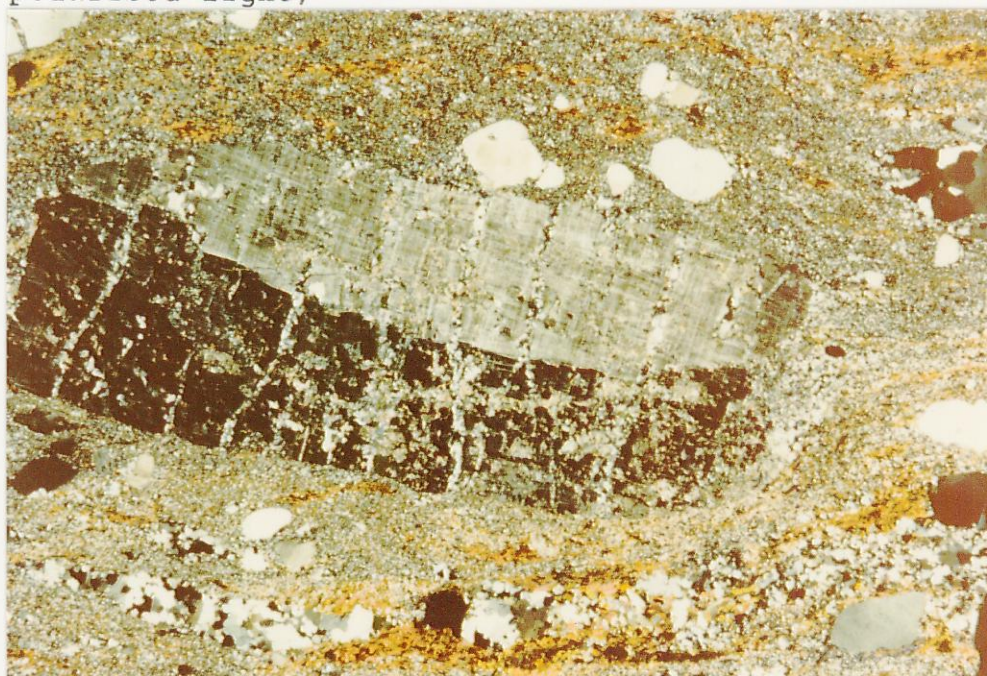


Plate 14. 6131 RS 89, 377.89 m: Bosanquet Formation. Blastomylonitic megacrystic rhyodacite. Coarse-grained, twinned and fractured microcline megacryst within a recrystallised quartz + feldspar matrix. Note tensile fractures are perpendicular to an elongation lineation, defined by a weak preferred-dimensional orientation of the quartz phenocrysts. Note elongate, dynamically recrystallised polycrystalline quartz phenocrysts. Field of view 16 mm x 11 mm. (Cross nicols)

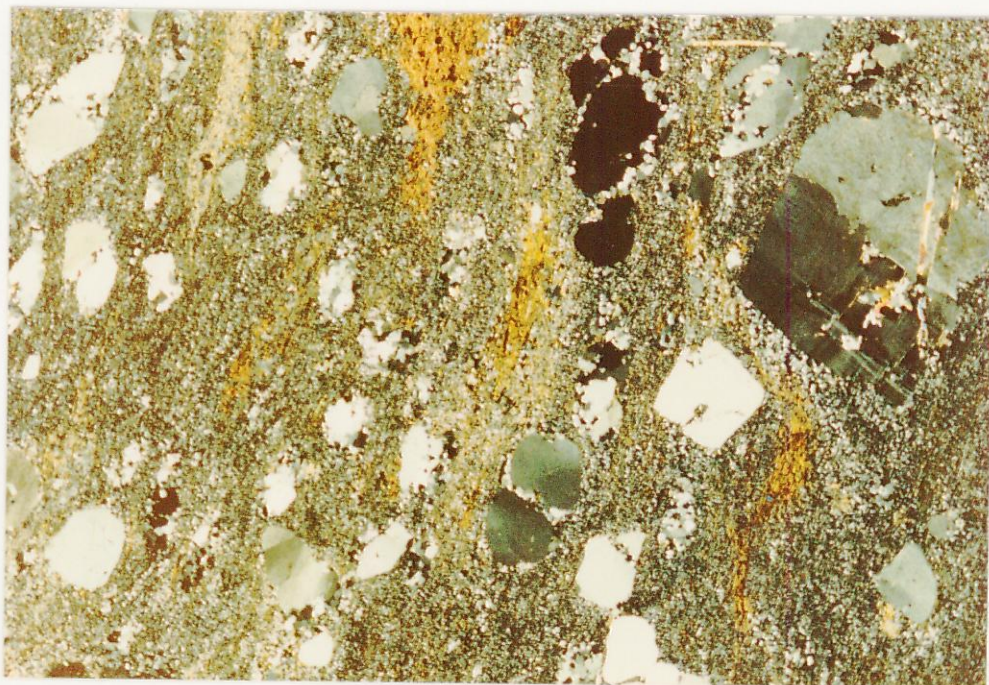


Plate 15. 6131 RS 90, 406.8 m: Bosanquet Formation. Protomylonitic phenocrystic rhyodacite. Note subrounded quartz and microcline phenocrysts within a fine-grained recrystallised matrix of quartz + feldspar + biotite. Field of view 16 mm x 11 mm. (Crossed nicols)

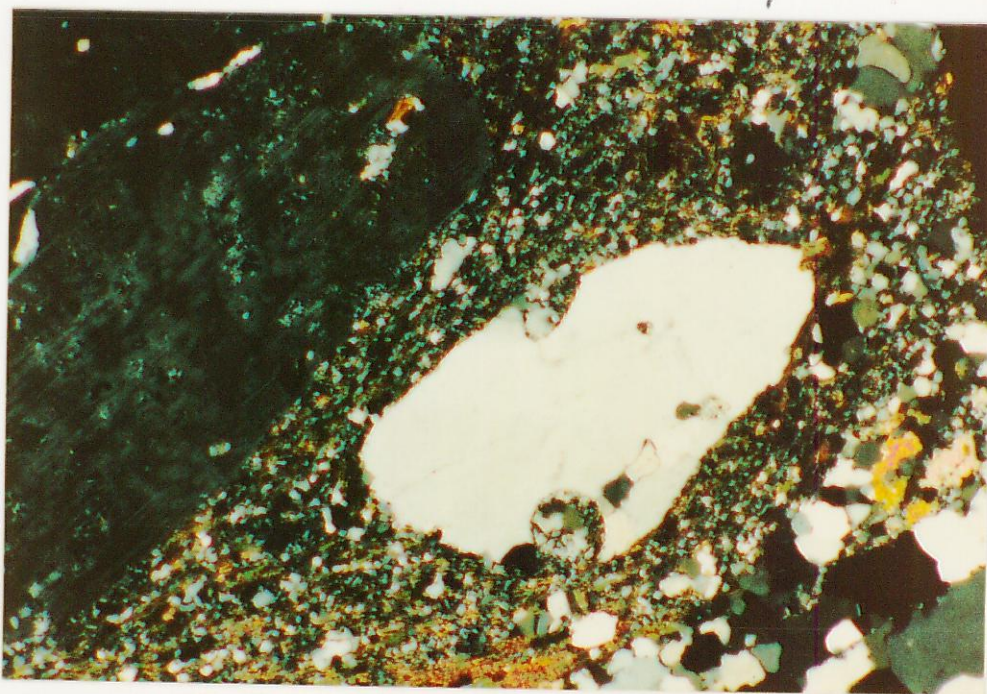


Plate 16. 6131 RS 85, 360.7 m: Bosanquet Formation. Quartz phenocryst within a recrystallised phenocrystic rhyodacite. Note relic corroded embayments preserved along the margins of the phenocryst. Field of view 2 mm x 1.4 mm. (Crossed nicols)

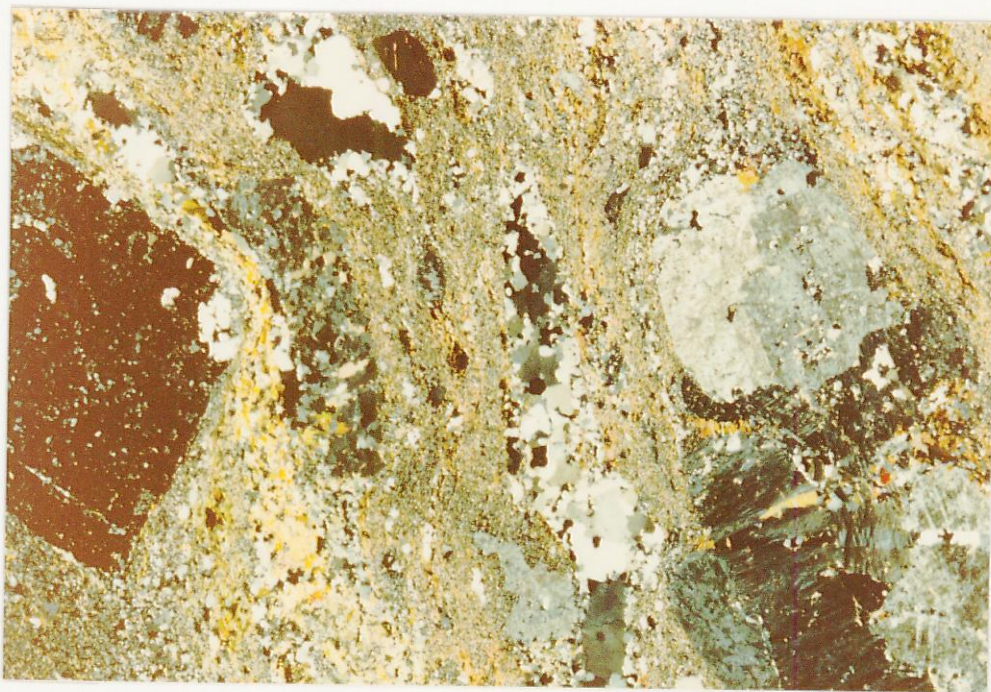


Plate 17. 6131 RS 85, 360.7 m: Bosanquet Formation. Recrystallised phenocrystic rhyodacite. Note recrystallised quartz phenocrysts (centre of photo), elongate parallel to a stretching lineation. Field of view 16 mm x 11 mm. (Crossed nicols)

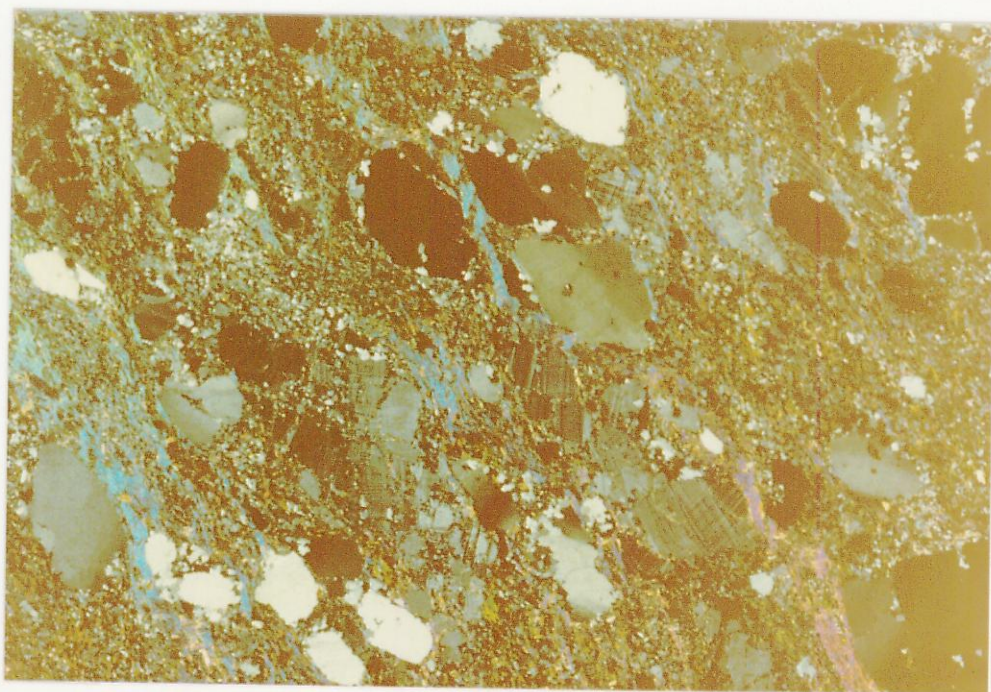


Plate 18. 6131 RS 76, 291.5 m: Bosanquet Formation. Blastomylonitic rhyodacite. Note elongation lineation defined by weakly-lenticular and highly-fractured microcline phenocrysts, rimmed by fine, dynamically-recrystallised grains. Field of view 16 mm x 11 mm. (Crossed nicols)



Plate 19. 6131 RS 76, 291.5 m: Bosanquet Formation. Fine- to medium-grained microcline + quartz + biotite + muscovite mylonitic rhyodacite. Note elongation lineation, defined by the preferred-dimensional orientation of relic quartz phenocrysts and biotite aggregate. Field of view 16 mm x 11 mm. (Crossed nicols)



Plate 20. 6131 RS 74, 188.95: Bosanquet Formation. Quartz + microcline+diopside calcsilicate. Note granoblastic-elongate texture and optically - continuous relics of originally coarse-grained diopside. Compare with calcsilicates of the Mt Shannan Iron Formation (Plate 4). Field of view 16 mm x 11 mm. (Crossed nicols)

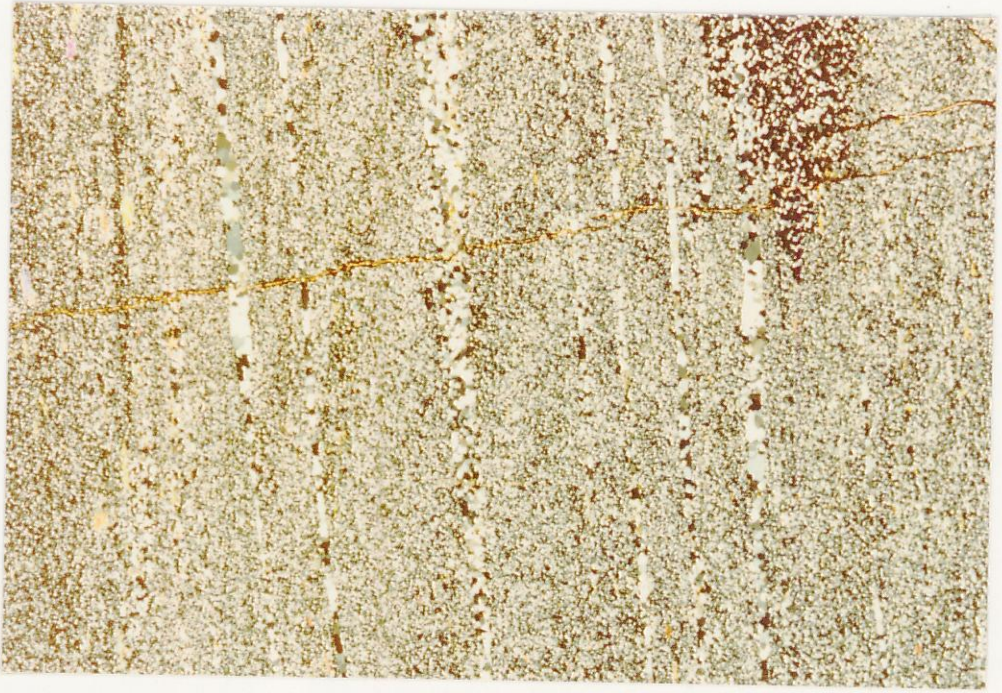


Plate 21. 6131 RS 96, 416.1 m: Mount Shannan Iron Formation. Quartz + magnetite gneiss. Note narrow quartz ribbons, axial-planar to tight folds visible within the magnetite-rich layers. Field of view 16 mm x 11 mm. (Plane polarised light)



Plate 22. 6131 RS 99, 420.9 m: Mt Shannan Iron Formation. Quartz + magnetite + amphibole gneiss. Note isoclinal folding of quartz-magnetite layering, with an axial-planar fabric defined by elongate blue-green hornblende + grunerite. Field of view 16 mm x 11 mm. (Plane polarised light)

APPENDIX III

GEOCHEMICAL DATA



The Australian
Mineral Development
Laboratories

Flemington Street, Frewville,
South Australia 5063
Phone Adelaide (08) 79 1662
Telex AA82520

Please address all
correspondence to
P.O. Box 114 Eastwood
SA 5063
In reply quote:

amdel

NATA CERTIFICATE

1/13/0 - AC 2069/87

28 November 1986

The Director General
SA Department of Mines & Energy
PO Box 151
EASTWOOD SA 5063

REPORT AC 2069/87

YOUR REFERENCE:

EX - 598, 12/07/0015

REPORT COMPRISING:

Cover sheet
Page X1
Pages I1 - I2
Pages G1 - G4

DATE RECEIVED:

18 November 1986

Approved Signatory:

Alan Ciplys

Manager, Geo-Analytical Services

for Dr William G. Spencer
General Manager
Applied Sciences Group

hy

Head Office:
Flemington Street, Frewville
South Australia 5063
Telephone (08) 79 1662
Telex: Amdel AA82520
Pilot Plant:
Osman Place
Thebarton, S.A.
Telephone (08) 43 5733
Telex: Amdel AA82725
Branch Laboratories:
Melbourne, Vic.
Telephone (03) 645 3093
Perth, W.A.
Telephone (09) 325 7311
Telex: Amdel AA94893
Sydney, N.S.W.
Telephone (02) 439 7735
Telex: Amdel AA20053
Townsville
Queensland 4814
Telephone (077) 75 1377



This laboratory is registered by the National Association of Testing Authorities, Australia. The test(s) reported herein have been performed in accordance with its terms of registration. This document shall not be reproduced except in full



Analysis code H1/1

Report AC 2069/87

Page I1

NATA Certificate

Results in percentages

	6131 73	RS 75	6131 76	RS 80	6131 85
SiO2	65.7	76.5	67.8	64.3	63.6
TiO2	0.80	0.17	0.23	0.65	0.59
Al2O3	18.0	10.2	15.7	15.6	13.7
Fe2O3	2.46	2.74	3.58	5.45	4.90
MnO	0.03	0.04	0.05	0.12	0.08
MgO	1.76	1.04	1.52	1.32	2.32
CaO	1.04	0.81	0.70	1.73	4.70
Na2O	1.90	1.35	1.20	2.38	1.55
K2O	6.85	5.25	8.70	8.25	6.15
P2O5	0.33	<0.010	0.07	0.11	0.07
LOI	2.14	0.85	1.45	1.11	2.14

Totals	101.0	98.9	101.0	101.0	99.8
--------	-------	------	-------	-------	------

BA	0.106	0.060	0.095	0.126	0.104
SR	0.006	0.005	0.006	0.008	0.016
CU	0.054	0.021	0.026	0.075	0.020
NI	<0.001	<0.001	<0.001	<0.001	<0.001
ZN	0.079	0.002	0.043	0.049	0.006
PB	<0.005	<0.005	<0.005	<0.005	<0.005
CR	0.022	<0.001	0.008	0.005	0.010
V	0.006	<0.001	<0.001	<0.001	<0.001
CO	0.011	0.020	0.013	0.007	0.012
ZR	0.142	0.059	0.084	0.120	0.116
LA	<0.002	<0.002	<0.002	<0.002	<0.002
Y	0.014	0.014	0.023	0.014	0.015
MO	<0.002	<0.002	<0.002	<0.002	<0.002

Total FE as Fe2O3



Analysis code H1/1

Report AC 2069/87

Page I2

NATA Certificate

Results in percentages

6131 RS
89

SiO2	67.9
TiO2	0.46
Al2O3	13.2
Fe2O3	3.56
MnO	0.08
MgO	0.80
CaO	1.15
Na2O	1.48
K2O	8.95
P2O5	0.07
LOI	0.93

Totals 98.6

BA	0.144
SR	0.005
CU	0.010
NI	<0.001
ZN	<0.001
PB	<0.005
CR	<0.001
V	<0.001
CO	0.013
ZR	0.095
LA	<0.002
Y	0.011
MO	<0.002

Total FE as Fe2O3



amdel

Analysis code X1

Report AC 2069/87

Page X1

NATA Certificate

Results in ppm

Sample	Rb	Cs	Nb	Ce	Th	U
6131 RS 73	98	<20	52	240	20	<4
6131 RS 75	125	<20	36	250	32	<4
6131 RS 76	200	<20	52	370	54	<4
6131 RS 80	130	<20	40	220	20	<4
6131 RS 85	110	<20	46	200	22	8
6131 RS 89	105	<20	38	190	26	<4
Detn limit	(2)	(20)	(4)	(20)	(4)	(4)



amdel

Analysis code A1/1,2
A2/3

Report AC 2069/87

Page G1

NATA Certificate

Results in ppm

Sample	Co	Cr	Cu	Ni	Pb	Zn	Ag
6131RS135	40	110	80	215	<5	78	<1
6131RS69	6	<10	5	<5	<5	150	<1
6131RS70	<5	<10	7	<5	20	120	<1
6131RS71	<5	<10	21	<5	10	70	<1
6131RS72	10	<10	3	<5	<5	190	<1
6131RS74	<5	<10	18	<5	38	42	<1
6131RS77	<5	10	10	<5	<5	76	<1
6131RS78	<5	<10	5	<5	28	32	<1
6131RS79	<5	<10	3	<5	6	100	<1
6131RS81	14	20	2	22	6	115	<1
6131RS82	14	20	3	24	<5	160	<1
6131RS83	14	15	20	22	<5	100	<1
6131RS84	22	15	68	32	255	375	<1
6131RS86	12	<10	34	20	6	150	<1
6131RS87	12	30	84	22	<5	130	<1
6131RS88	10	30	10	16	6	60	<1
6131RS90	<5	<10	8	<5	<5	42	<1
6131RS91	6	10	46	6	<5	30	<1
6131RS92	8	10	13	14	<5	34	<1
6131RS93	6	10	54	8	6	25	<1
6131RS94	8	10	27	10	<5	25	<1
6131RS95	<5	15	2	6	8	22	<1
6131RS96	<5	<10	6	<5	<5	29	<1
6131RS97	<5	15	110	<5	<5	15	<1
6131RS98	10	15	5	18	<5	21	<1
6131RS99	<5	10	12	<5	<5	16	<1
6131RS100	8	15	4	16	<5	35	<1
6131RS101	8	15	26	8	<5	22	<1
6131RS102	<5	<10	5	<5	<5	12	<1
6131RS103	<5	<10	3	<5	<5	15	<1
6131RS104	64	370	100	195	<5	120	<1
6131RS105	6	10	8	12	6	28	<1
6131RS106	<5	<10	6	<5	<5	10	<1
6131RS107	8	10	5	12	<5	30	<1
Detn limit	(5)	(10)	(2)	(5)	(5)	(2)	(1)



amdel

Analysis code A1/1,2
A2/3

Report AC 2069/87

Page G2

NATA Certificate

Results in ppm

Sample	Co	Cr	Cu	Ni	Pb	Zn	Ag
6131RS108	48	190	96	200	<5	125	<1
6131RS109	12	10	4	52	<5	40	<1
6131RS110	6	<10	5	8	<5	21	<1
6131RS111	10	25	540	22	<5	46	<1
6131RS112	<5	<10	3	6	<5	18	<1
6131RS113	<5	<10	12	<5	<5	12	<1
6131RS114	135	190	165	290	<5	200	<1
6131RS115	8	15	10	50	<5	22	<1
6131RS116	42	220	115	250	<5	56	<1
6131RS117	46	130	105	165	<5	110	<1
6131RS118	<5	<10	37	10	<5	16	<1
6131RS119	6	10	23	12	<5	22	<1
6131RS120	8	<10	44	10	<5	14	<1
6131RS121	6	<10	8	6	<5	16	<1
6131RS122	<5	10	9	6	6	18	<1
6131RS123	135	380	150	275	6	45	<1
6131RS124	72	290	145	250	<5	105	<1
6131RS125	68	260	105	260	<5	88	<1
6131RS126	80	310	110	495	<5	74	<1
6131RS127	50	170	105	345	<5	72	<1
6131RS128	18	30	26	46	<5	62	<1
6131RS129	12	40	18	26	<5	38	<1
6131RS130	68	190	86	180	<5	74	<1
6131RS131	8	<10	180	10	6	29	<1
6131RS132	10	15	32	42	<5	33	<1
6131RS133	40	160	105	245	<5	64	<1
6131RS134	48	240	41	330	<5	78	<1
Detn limit	(5)	(10)	(2)	(5)	(5)	(2)	(1)



amdel

Analysis code A1/1,2
A2/3

Report AC 2069/87

Page G3

NATA Certificate

Results in ppm

Sample	Mo	V	Au
6131RS135	3	190	<0.01
6131RS69	4	25	<0.01
6131RS70	6	30	<0.01
6131RS71	3	30	<0.01
6131RS72	2	45	<0.01
6131RS74	7	30	<0.01
6131RS77	5	20	<0.01
6131RS78	5	<20	<0.01
6131RS79	6	35	<0.01
6131RS81	3	95	<0.01
6131RS82	3	80	<0.01
6131RS83	3	95	<0.01
6131RS84	4	65	<0.01
6131RS86	4	35	<0.01
6131RS87	5	75	<0.01
6131RS88	3	75	<0.01
6131RS90	6	20	<0.01
6131RS91	3	45	<0.01
6131RS92	2	60	<0.01
6131RS93	2	60	<0.01
6131RS94	1	60	<0.01
6131RS95	5	45	<0.01
6131RS96	<1	35	<0.01
6131RS97	2	20	<0.01
6131RS98	<1	75	<0.01
6131RS99	<1	30	<0.01
6131RS100	1	80	<0.01
6131RS101	<1	40	<0.01
6131RS102	<1	<20	<0.01
6131RS103	<1	30	<0.01
6131RS104	2	430	<0.01
6131RS105	<1	45	<0.01
6131RS106	<1	35	<0.01
6131RS107	<1	40	<0.01

Detn limit (1) (20) (0.01)



amdel

Analysis code A1/1,2
A2/3

Report AC 2069/87

Page G4

NATA Certificate

Results in ppm

Sample	Mo	V	Au
6131RS108	<1	370	<0.01
6131RS109	<1	40	<0.01
6131RS110	1	40	<0.01
6131RS111	<1	70	<0.01
6131RS112	<1	30	<0.01
6131RS113	<1	25	<0.01
6131RS114	5	590	<0.01
6131RS115	2	35	<0.01
6131RS116	<1	160	<0.01
6131RS117	<1	240	<0.01
6131RS118	1	30	<0.01
6131RS119	<1	50	<0.01
6131RS120	<1	40	<0.01
6131RS121	<1	25	<0.01
6131RS122	<1	20	<0.01
6131RS123	1	540	<0.01
6131RS124	3	400	<0.01
6131RS125	<1	250	<0.01
6131RS126	3	270	<0.01
6131RS127	<1	210	<0.01
6131RS128	<1	110	<0.01
6131RS129	1	150	<0.01
6131RS130	<1	370	<0.01
6131RS131	1	45	<0.01
6131RS132	<1	90	<0.01
6131RS133	<1	95	<0.01
6131RS134	<1	220	<0.01

Detn limit (1) (20) (0.01)

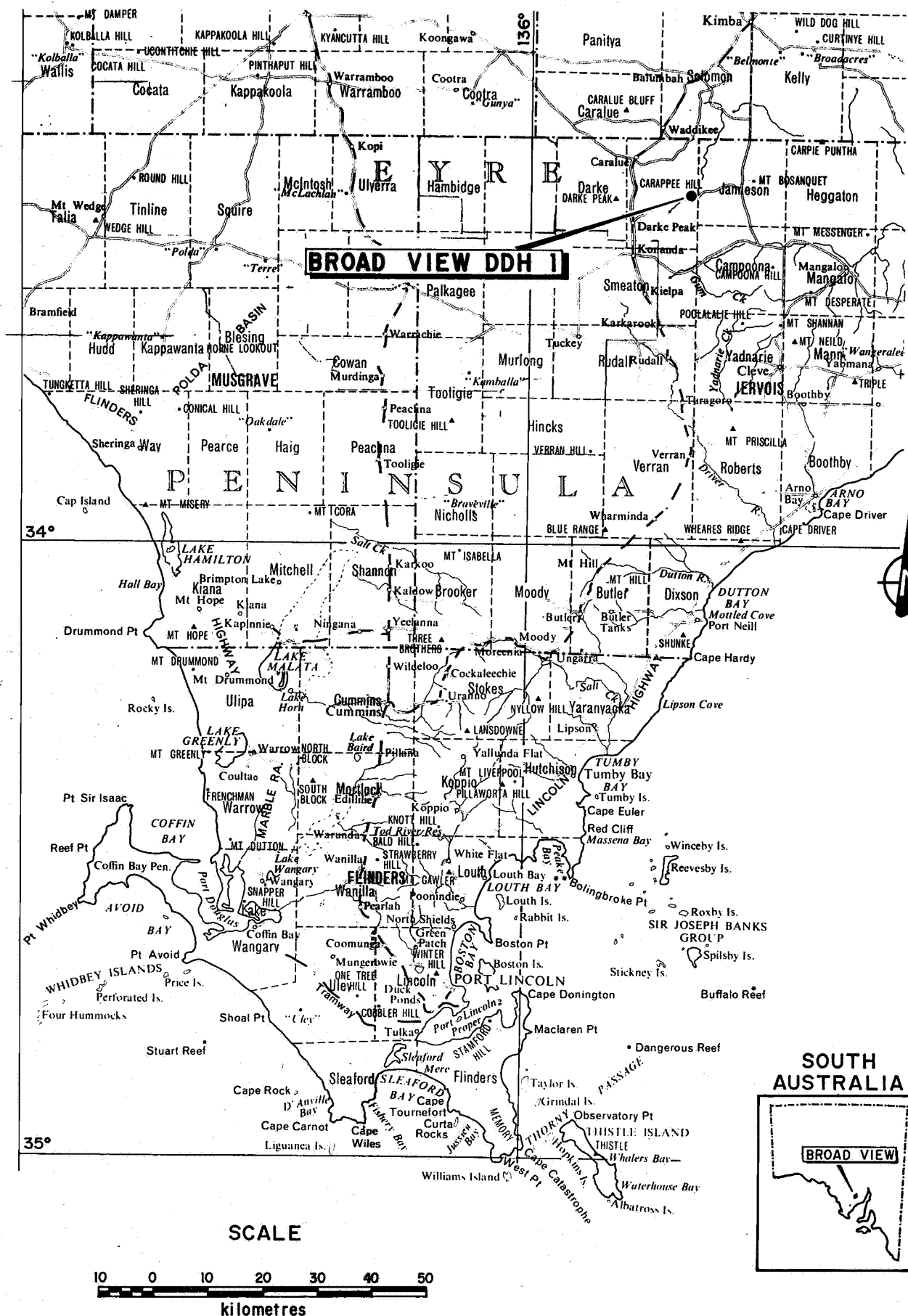

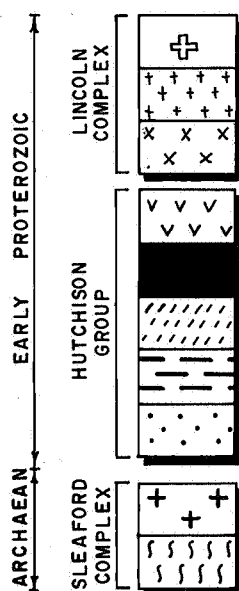
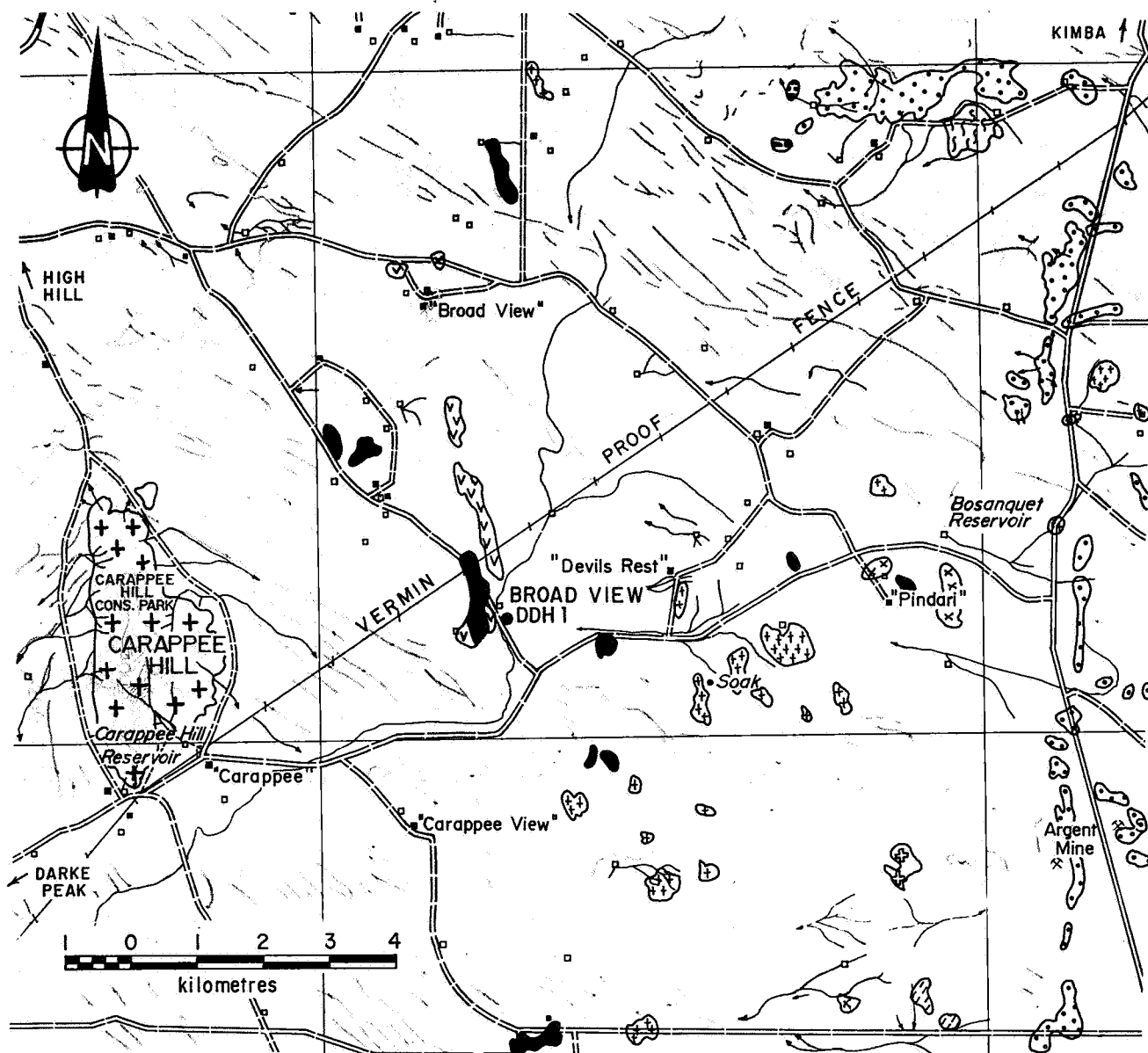


FIG. 1

	DEPARTMENT OF MINES AND ENERGY SOUTH AUSTRALIA		COMPILED L. Rankin	20-8-87 C.D.O. DATE
	BROAD VIEW DDH 1 WELL COMPLETION REPORT WELL No. 6131002SW00124		DRAWN R. Bird	SCALE 1:1000000
	LOCALITY PLAN		DATE May 1987	PLAN NUMBER S19321
			CHECKED	



Carpa Granite equivalent
 Middlecamp Granite equivalent
 Undifferentiated Lincoln Complex granite/gneiss
 Bosanquet Formation
 Mt. Shannan Iron Formation
 Mangalo Schist
 Lower iron formation
 Warrow Quartzite
 Tabular feldspar granite gneiss
 Quartz + feldspar + garnet gneiss

FIG. 2



DEPARTMENT OF MINES AND ENERGY
 SOUTH AUSTRALIA

BROAD VIEW DDH 1 WELL COMPLETION REPORT

WELL No. 6131002SW00124

OUTCROP GEOLOGY

COMPILED
 L. Rankin

DRAWN
 R. Bird

DATE
 May 1987

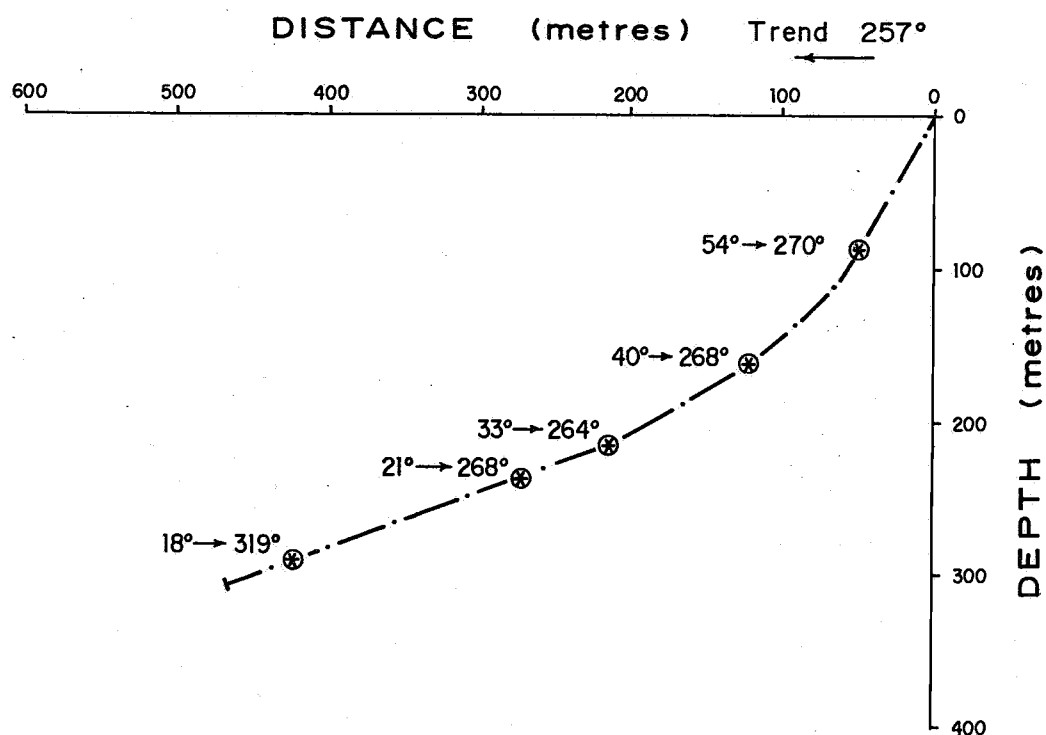
CHECKED

20-8-87
 C.D.O. DATE

SCALE 1:100 000


PLAN NUMBER

S19322



⊗ Tropari test site

FIG. 3

 DEPARTMENT OF MINES AND ENERGY SOUTH AUSTRALIA	COMPILED L. Rankin	<i>LR</i> 20-8-87 C.D.O. DATE
	DRAWN R. Bird	SCALE 1:5000
	DATE May 1987	PLAN NUMBER
	CHECKED	S19323

BROAD VIEW DDH 1 WELL COMPLETION REPORT
WELL No. 6131002SW00124

DRILLHOLE DEVIATION GRAPH

CORE DESCRIPTION

DEPTH . . 578.6 m.

INCLINATION 60° (initial)

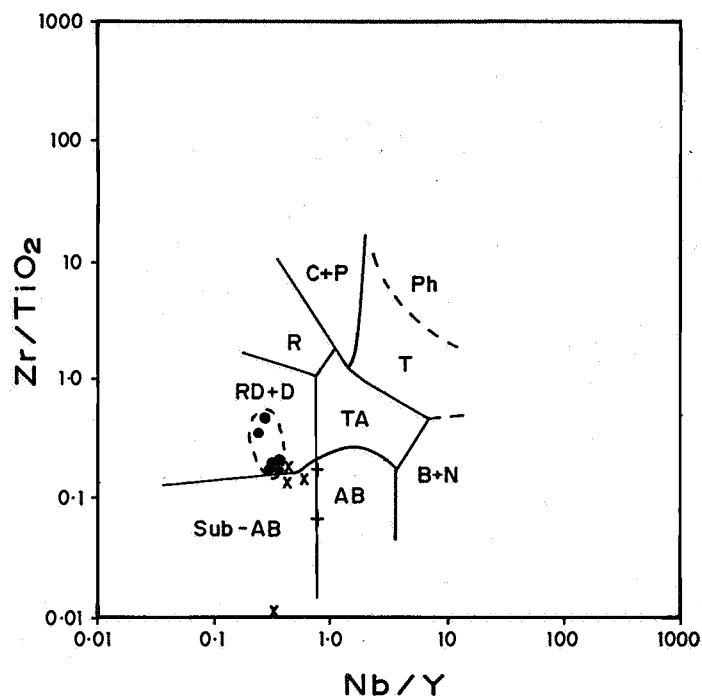
LOGGED BY . R.B.F. & L.R.R.

DECLINATION 257°

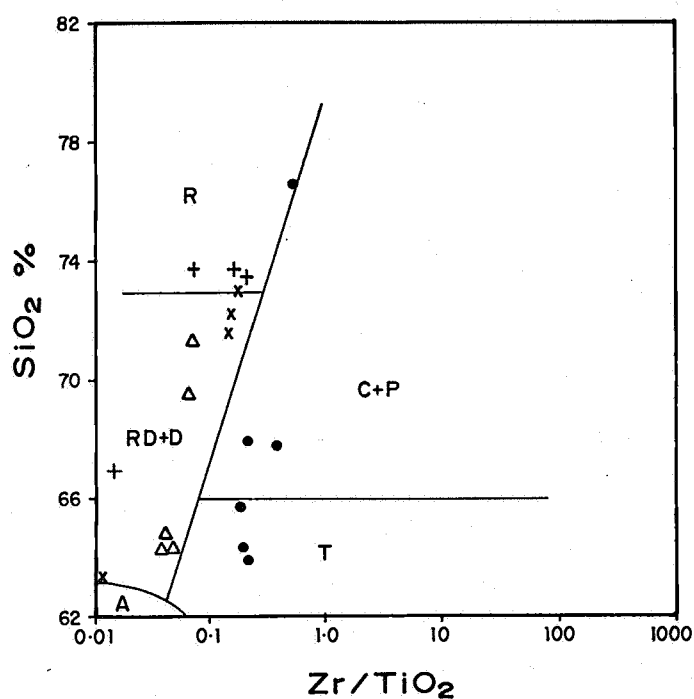
REFERENCE

DATE DRILLED 2/8/86 - 14/10/86

DEPTH (m)		GRAPHIC LOG	DESCRIPTION
CAINOZOIC	26.2		Green to limonitic yellow sandy clays and clay-rich sands. Grades into coarse grained fluvialite gravels and conglomerate with abundant well-rounded quartzite pebbles.
	50		Grey, recrystallised rhyodacite (q + micr. + bi + musc.) with abundant bluish quartz megacrysts (<3mm) and feldspar megacrysts (<10mm). The rhyodacite has been deformed and recrystallised, with development of an intense anastomosing foliation, mylonitic in character. Abundant quartz veins, <15 cm wide, commonly associated with minor sulphides. Proportion of feldspar megacrysts increases towards the base.
	100		Well-banded, grey-green, q + fsp + hbl + bi + ca + di calcsilicate gneiss. Contains thin (<10cm) bands of recrystallised rhyodacite and abundant quartz veins.
	112.3		Grey, recrystallised, well foliated rhyodacite (as above) contains minor diopside-rich calcsilicate layers. Foliation is variable in intensity, with a variable-intensity elongation lineation.
	127.6		Well-banded, fine-grained, diopside-rich calcsilicate gneiss
	150		Grey, well-foliated, recrystallised rhyodacite (as above). Foliation varies from gneissic to blastomylonitic in character, with reduction in size and attenuation of megacrysts. Contains minor calcsilicate layers.
	187.25		Fine-grained, grey-green di. + act. + ca - bearing calcsilicate gneiss. Interlayered with fine-grained recrystallised rhyodacite.
	189.15		Grey, well-foliated recrystallized rhyodacite (as above).
	200		Fine-to-coarse-grained megacrystic, recrystallised rhyodacite. Contains abundant subhedral microcline megacrysts (<2cm) within a fine-grained matrix of q + fsp + bi. Occasional embayed quartz phenocrysts. Minor thin bands of calcsilicate gneiss.
	250		Fine-grained, grey calcsilicate gneiss with interlayered recrystallised rhyodacite. Abundant pyrite.
BOSANQUET FORMATION	300		Fine-grained q + fsp + bi gneiss.
	302.2		Q + fsp + di calcsilicate gneiss. Contains fine-grained bands of inclusion-rich plagioclase.
	305.5		Grey, well foliated, recrystallised megacrystic rhyodacite (as above).
	315.4		Dark brown-grey q + fsp + bi schist.
	346.0		Grey, well-foliated, recrystallised rhyodacite (as above)
	350		Interlayered q + mt + grun iron formation, fine-grained quartzite, mt + hbl calcsilicate and garnetiferous mt + ca + act/hbl + di + grun calcsilicate.
	351.25		Well-banded ca + act./hbl. + grun + di + qa calcsilicate gneiss.
	361.05		Poorly-banded ca + q + di calcsilicate gneiss. Banding is contorted and disrupted
	362.0		Banded q + mt + grun schist + banded di + hbl + ca. gneiss.
	364.6		Streaky-foliated ca + di + bi gneiss and bi + ca. schist
EARLY PROTEROZOIC	400		Mt. + act + ga + ca gneiss, with bands of q + ga + bi, ca + mt + chl., ga + bi + act.
	400.33		Well-banded di + ca + amph. - rich calcsilicate gneiss.
	401.0		Poorly-banded ca + q + di calcsilicate gneiss, with interlayered bi + ca. schist.
	407.8		Well-banded calcsilicate gneiss with abundant magnetite-rich layers
	414.98		Poorly-banded ca + q + di calcsilicate gneiss (as above)
	437.75		Bi + ca. schist. Schistosity is moderately anastomosing.
	450.2		Streaky-foliated ca + di + amph calcsilicate gneiss with minor ca + bi. schist. Schistosity is weakly anastomosing.
	456.85		Mt. + hbl. + bi + ca. calcsilicate gneiss, well banded. Minor quartz-rich layers.
	462.86		Streaky-foliated ca + di + amph calcsilicate gneiss (as above).
	464.20		Well-banded bi + ca + hbl calcsilicate schist, with abundant pyrite.
MT. SHANNAN IRON FORMATION	471.55		Streaky-foliated ca + di + amph calcsilicate gneiss (as above).
	473.60		Well-banded bi + ca + hbl calcsilicate schist, with abundant pyrite.
	478.00		Streaky-foliated ca + di + amph calcsilicate gneiss (as above).
	482.40		Well-banded bi + ca + hbl calcsilicate schist, with abundant pyrite.
	492.60		Streaky-foliated ca + di + amph calcsilicate gneiss (as above).
	497.80		Well-banded bi + ca + hbl calcsilicate schist, with abundant pyrite.
	499.80		Streaky-foliated ca + di + amph calcsilicate gneiss (as above).
	534.55		Well-banded bi + ca + hbl calcsilicate schist, with abundant pyrite.
	539.3		Streaky-foliated ca + di + amph calcsilicate gneiss (as above).
	550		Well-banded bi + ca + hbl calcsilicate schist, with abundant pyrite.



- - Bosanquet Formation rhyodacites
- x - Myola Volcanics rhyolites
- + - Tidnamurkana Volcanics
- Δ - McGregor Volcanics



- A - andesites
- AB - alkaline basalts
- Sub-AB - sub-alkaline basalts
- B+N - basanites and nephelinites
- C+P - comendites and pantellerites
- Ph - phonolites
- R - rhyolites
- RD+D - rhyodacites and dacites
- T - trachytes
- TA - trachyandesites

Note:

The igneous discrimination fields are adapted from Floyd and Winchester (1978)

FIG. 5



DEPARTMENT OF MINES AND ENERGY
SOUTH AUSTRALIA

BROAD VIEW DDH 1 WELL COMPLETION REPORT
WELL No. 6131002SW00124

Zr/TiO₂ VS Nb/Y AND SiO₂ VS Zr/TiO₂
DIAGRAMS

COMPILED
L. Rankin

DRAWN
R. Bird

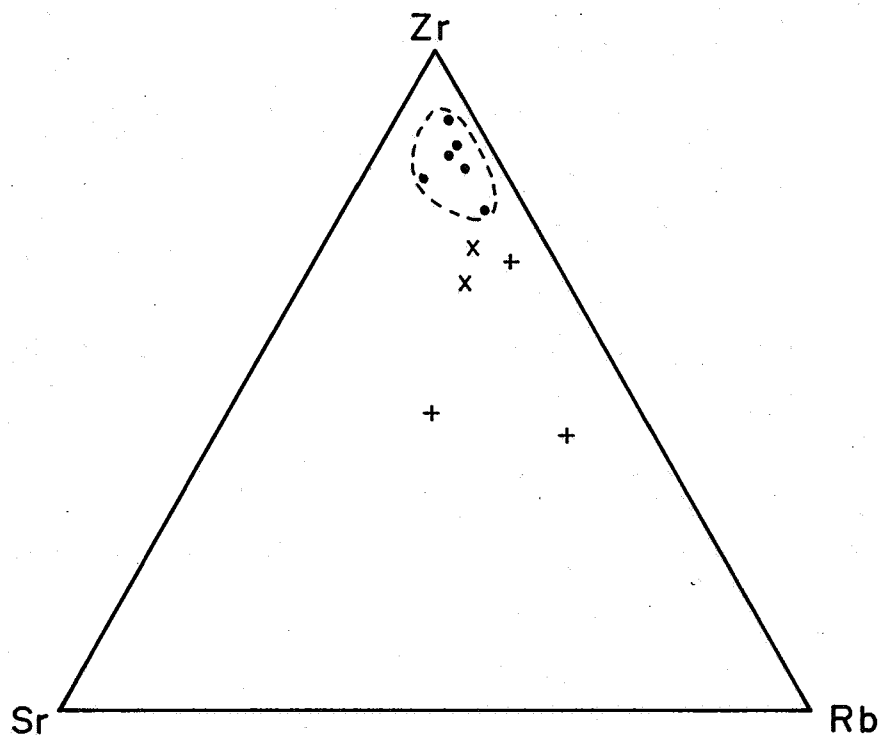
DATE
May 1987
CHECKED

20.8.87
C.D.O. DATE

SCALE As shown



PLAN NUMBER

S19325



- - Bosanquet Formation rhyodacites
- x - Myola Volcanics rhyolites
- + - Tidnamurkana Volcanics

FIG. 6

 DEPARTMENT OF MINES AND ENERGY SOUTH AUSTRALIA	COMPILED L. Rankin	 20.0.87 C.D.O. DATE
	DRAWN R. Bird	SCALE -
	DATE May 1987	PLAN NUMBER
	CHECKED	S19326

BROAD VIEW DDH 1 WELL COMPLETION REPORT
WELL No. 6131002SW00124
Zr VS Sr VS Rb TRIANGULAR DIAGRAM

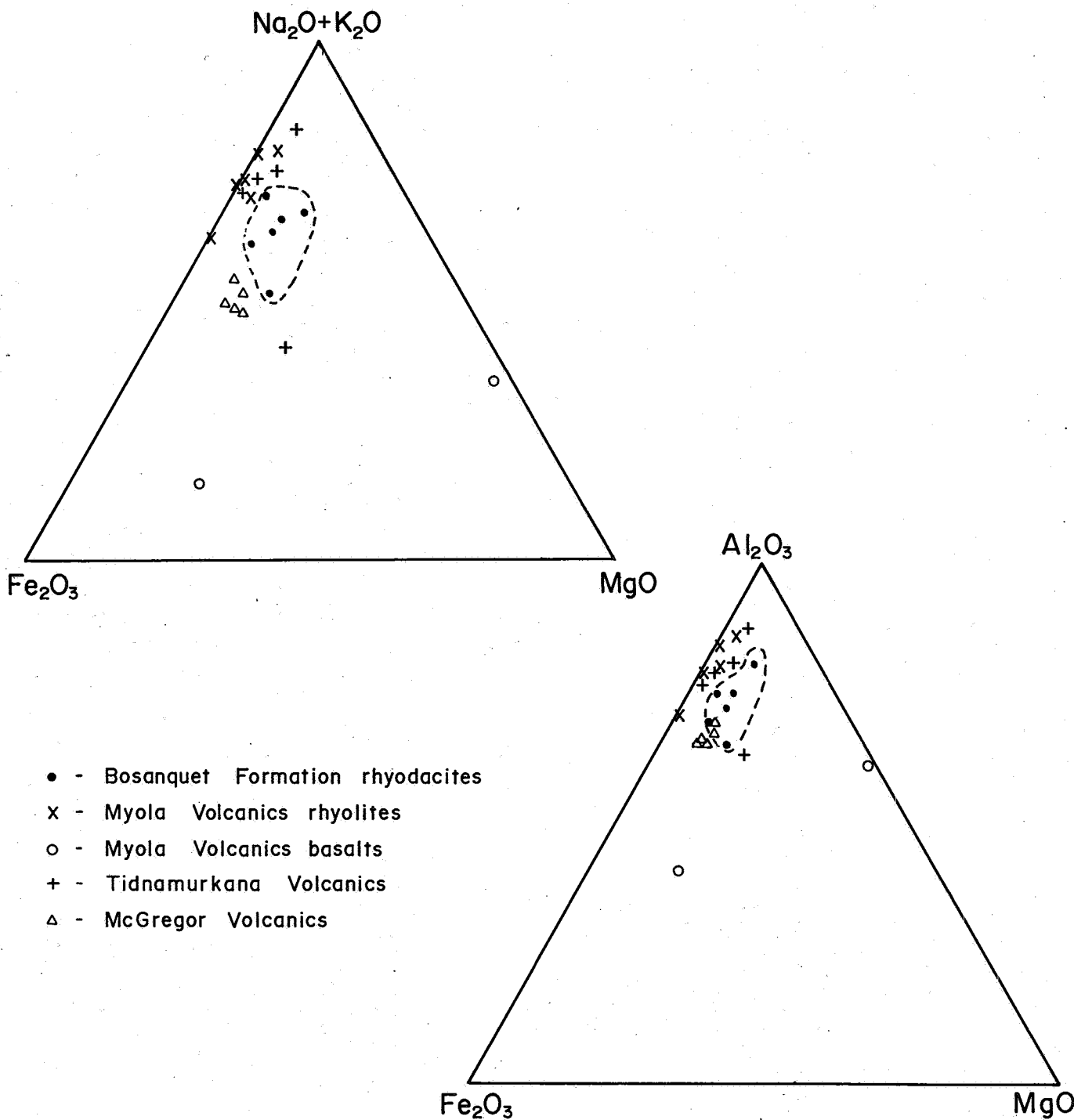

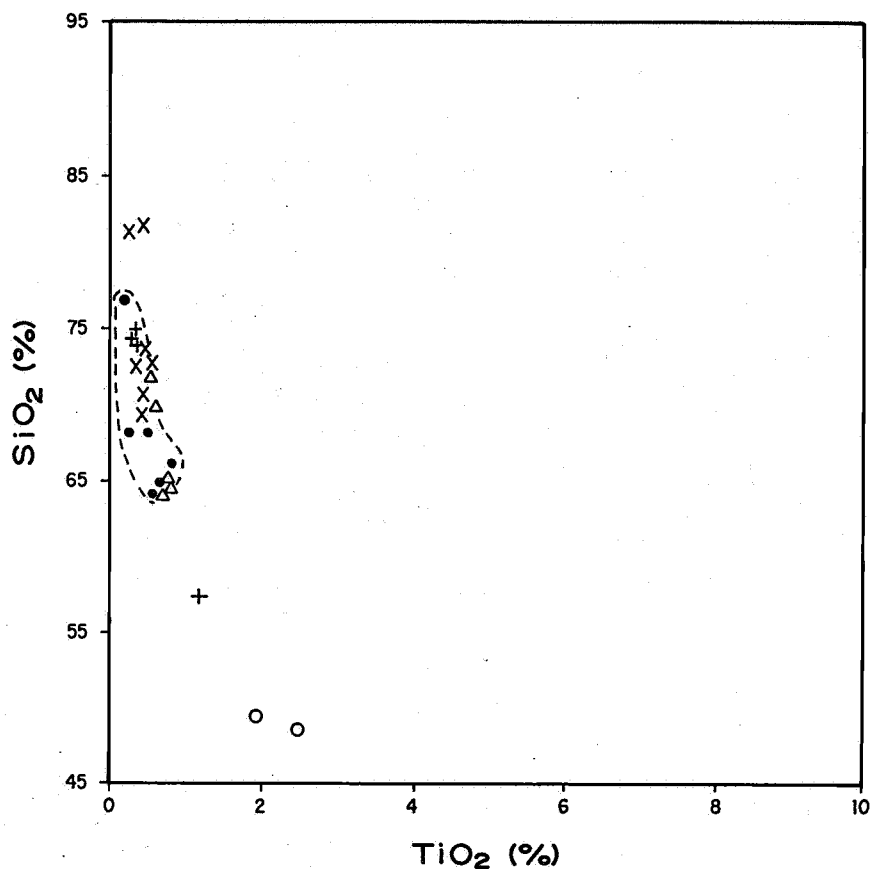


FIG. 7

	DEPARTMENT OF MINES AND ENERGY SOUTH AUSTRALIA		COMPILED L. Rankin	<i>LR</i> 20.8.87 C.D.O. DATE
	BROAD VIEW DDH 1 WELL COMPLETION REPORT WELL No. 6131002SW00124		DRAWN R. Bird	SCALE -
	AFM AND Al₂O₃ VS Fe₂O₃ VS MgO TRIANGULAR DIAGRAMS		DATE May 1987	PLAN NUMBER S19327
			CHECKED	



- - Bosanquet Formation rhyodacites
- x - Myola Volcanics rhyolites
- o - Myola Volcanics basalts
- + - Tidnamurkana Volcanics
- Δ - McGregor Volcanics

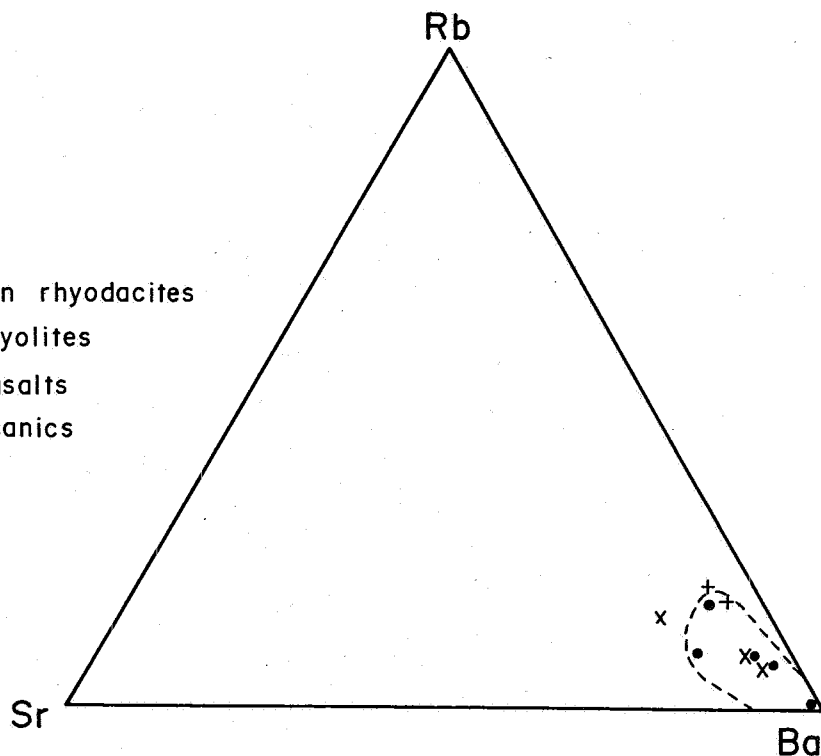


FIG. 8



DEPARTMENT OF MINES AND ENERGY
SOUTH AUSTRALIA

BROAD VIEW DDH 1 WELL COMPLETION REPORT
WELL No. 6131002SW00124

COMPILED
L. Rankin

LR 20-8-87
C.D.O. DATE

DRAWN
R. Bird

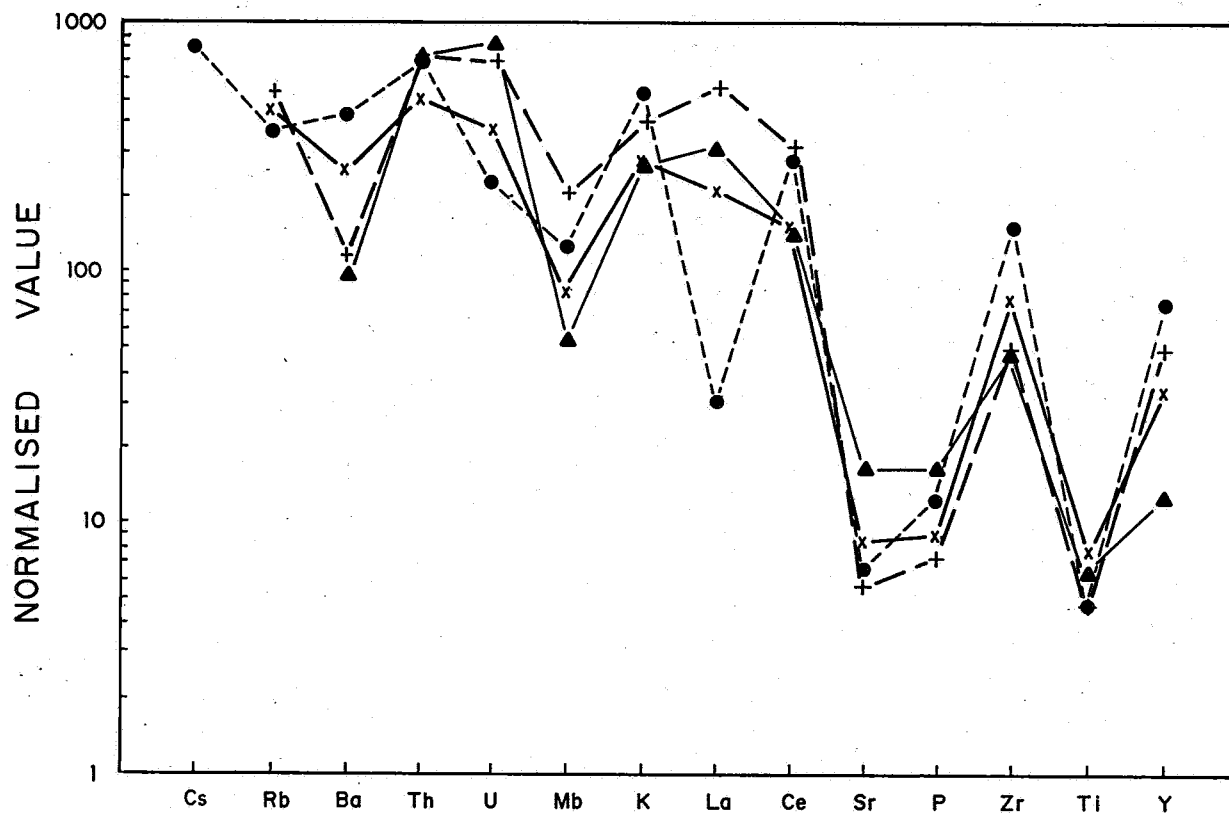
SCALE As shown

DATE
May 1987

PLAN NUMBER


CHECKED

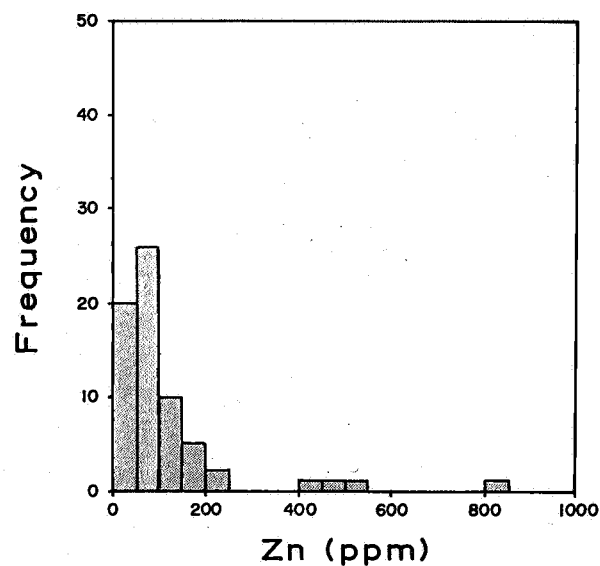
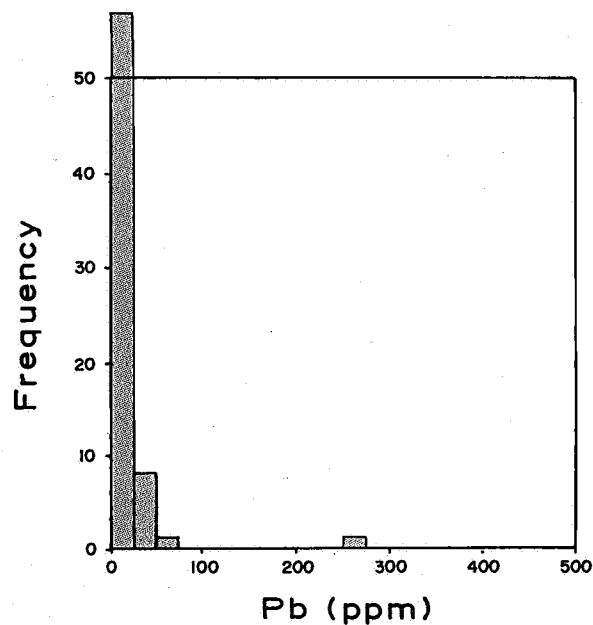
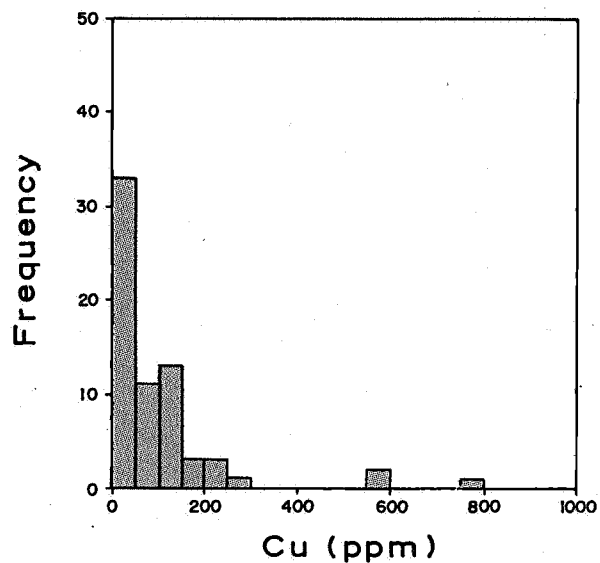
S19328



Each trend is an average of all available samples for each suite.


FIG. 9

	DEPARTMENT OF MINES AND ENERGY SOUTH AUSTRALIA		COMPILED L. Rankin	<i>LR</i> 20-6-87 C.D.O. DATE
	BROAD VIEW DDH 1 WELL COMPLETION REPORT WELL No. 6131002SW00124		DRAWN R. Bird	SCALE As shown
	CHONDRITE-NORMALISED DIAGRAM		DATE June 1987	PLAN NUMBER
			CHECKED	S19329



Base metal concentrations within the Bosanquet Fmn. and Mt. Shannon Iron Fmn.

FIG. 10

 DEPARTMENT OF MINES AND ENERGY SOUTH AUSTRALIA	COMPILED L. Rankin	<i>UR</i> 20.8.87 C.D.D. DATE
	DRAWN R. Bird	SCALE As shown
	DATE June 1987	PLAN NUMBER
	CHECKED	S19331

BROAD VIEW DDH 1 WELL COMPLETION REPORT
WELL No. 6131002SW00124
**HISTOGRAM GRAPHS OF Cu, Pb AND
Zn CONCENTRATIONS**

S.A.D.M.E.

COMPUTERISED BOREHOLE LOGGING

BOREHOLE PROJECT NO.

BROAD VIEW NO. 1

BOROHOLE UNIT NO.

VERTICAL SCALE 1: 500

DEPTH LOGGED 488.00 M.

DATE LOGGED 18/10/86

DATE PROCESSED 31/12/87

S.A.D.M.E.

DARKE PEAK AREA

S.A.D.M.E. JOB #

AUST. MAP GRID REF.

1:100,000 REF. SHEET NO.

OPERATOR N. J. R. G. R.

DATE ABOVE GROUND LEVEL 0.50 M.

CASING DEPTH 210.0 M.

LOGGING SPEEDS AND LINEARITIES

16" NORMAL RES. (OHM-M)

10 1100

04" NORMAL RES. (OHM-M)

10 1100

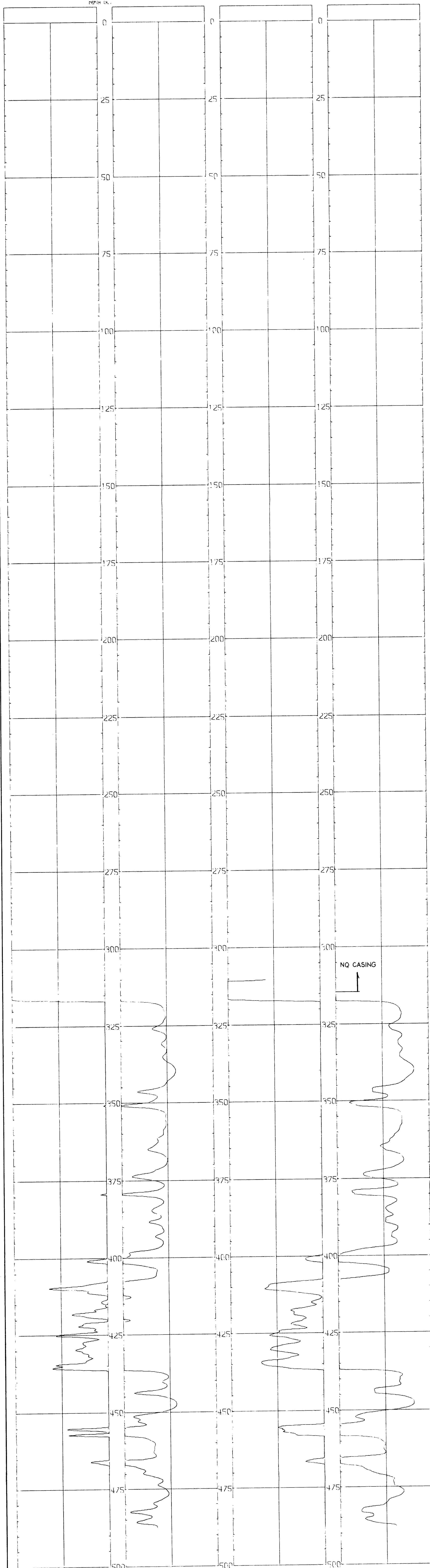
16" NORMAL RES. (OHM-M)

1000 100100

04" NORMAL RES. (OHM-M)

1000 100100

DEPTH IN.



16" NORMAL RES. (OHM-M)

1000 100100

04" NORMAL RES. (OHM-M)

1000 100100

16" NORMAL RES. (OHM-M)

10 1100

04" NORMAL RES. (OHM-M)

10 1100